Estudios Geológicos
enero-junio 2019, 75(1), e089
ISSN-L: 0367-0449
https://doi.org/10.3989/egeol.43377.507

Miocene syntectonic fluvial and lacustrine sedimentation linked to a fault-parallel buttress syncline in the Nigüella sector (NW Iberian Range)

Sedimentación fluvial y lacustre sintectónica ligada a un sinclinal de "buttressing" paralelo a una falla en el sector de Nigüella (NW Cordillera Ibérica)

N. Santos Bueno[1,3], C. Arenas Abad[1,3], A. Gil Imaz[2,3]

[1] Stratigraphy division. Department of Earth Sciences. University of Zaragoza. 50009 Zaragoza, Spain. Email: santosbuenonerea@gmail.com, carenas@unizar.es; ORCID ID: http://orcid.org/0000-0002-2876-9554, http://orcid.org/0000-0002-4212-0524

[2] Geodynamics (Structural Geology) division. Department of Earth Sciences. University of Zaragoza. 50009 Zaragoza, Spain. ORCID ID: http://orcid.org/0000-0001-6110-1081

[3] Institute for Research on Environmental Sciences of Aragón (IUCA) and Geotransfer group, University of Zaragoza. 50009 Zaragoza, Spain

ABSTRACT

This paper discusses the sedimentary evolution of an area with Neogene fluvial and lacustrine deposits in the northwestern part of the Iberian Range, and its relation to the effects of Alpine compressional tectonics affecting a major, formerly extensional fault. Stratigraphic analyses allow characterizing three tectosedimentary units. Units 1 and 2 are dominated by clastics lithofacies, and are separated by an unconformity and the correlative conformity. Unit 3 is formed of tufa and micritic limestones and represents a sharp lithological change throughout the area. Total thickness is 120 m. These units are involved in two NNW-SSE Alpine trending, kilometric-scale structures: 1) the Nigüella fault, that put into contact Triassic rocks, in the footwall, with Cenozoic rocks, in the hanging-wall, and 2) the Nigüella syncline, subparallel to this fault, with strata dips between 19° up to 70°. In units 1 and 2, four facies associations represent deposition in proximal to middle alluvial fans, from local reliefs, and a braided fluvial system with limited floodplain, running southward; both environments record minor fluvial and lacustrine carbonate deposition. Three other facies associations represent dominant carbonate deposition, either palustrine-fluvial-lacustrine or lacustrine settings. In the three units, oncoid and phytoclast rudstones formed in shallow, low-sinuosity channels and pools with extensive tufaceous palustrine areas, where hydrophilous plants throve. In contrast, micritic limestones with ostracods and marls correspond to offshore dominant carbonate lacustrine deposition in still and permanent lakes. Thus the overall sedimentary system evolved from dominant alluvial-fluvial to dominant lacustrine carbonate environments through time. These facts, along with calcrete development in Units 1 and 2, indicate increasing precipitation and probably the passage to a hydrologically-closed lake basin through time. The Nigüella fault played as a normal fault at the early Jurassic and during the Cenozoic compression it promoted the formation of a hanging-wall syncline basin through buttressing of the NE block against the fault. This scenario conditioned the distribution and extent of the Miocene lithofacies through space and time, and the location of depocentres. Decreasing tectonic activity through the studied interval favoured fluvial incision, capture of the

Recibido el 4 de octubre de 2018 / Aceptado el 17 de enero de 2019 / Publicado online el 13 de mayo de 2019

Citation / Cómo citar este artículo: Santos Bueno, N. et al. (2019). Miocene syntectonic fluvial and lacustrine sedimentation linked to a fault-parallel buttress syncline in the Nigüella sector (NW Iberian Range). Estudios Geológicos 75(1): e089. https://doi.org/10.3989/egeol.43377.507

Mesozoic aquifer, and then outflow of ground water rich in Ca^{2+} and HCO^{-}_{3}, thus favouring widespread carbonate deposition, and finally the expansion of the lake area.

Keywords: Alluvial deposits; Lacustrine carbonates; Tufa; Syntectonic deposition; Buttressing; Neogene.

RESUMEN

En este artículo se discute la evolución sedimentaria del relleno neógeno de un área situada en la parte Noroeste de la Cordillera Ibérica que presenta depósitos fluviales y lacustres, y su relación con la tectónica alpina compresiva que afectó a una falla anteriormente extensional. Los análisis estratigráficos permiten caracterizar tres unidades tectosedimentarias, con un espesor total de 120m. Las Unidades 1 y 2 están formadas dominantemente por litofacies clásticas, y están separadas por una discordancia y su correlativa conformidad. La Unidad 3 está formada por calizas tobáceas y micríticas, y representa un salto litológico brusco con la Unidad 2 en toda su extensión. Estas unidades están involucradas en dos estructuras de escala kilométrica con dirección alpina NNW-SSE: 1) la Falla de Nigüella, que pone en contacto materiales triásicos con cenozoicos en los bloques levantado y hundido, respectivamente, y 2) el Sinclinal de Nigüella, subparalelo a la falla anterior, con buzamiento de estratos entre 19º y 70º. En las unidades 1 y 2, cuatro asociaciones de facies sedimentarias representan el depósito en áreas proximales y medias de abanicos aluviales, procedentes de relieves locales, y un sistema fluvial braided con reducida llanura de inundación, procedente del Norte. Ambos ambientes registran sedimentación carbonática fluvial y lacustre. Otras tres asociaciones de facies representan el depósito dominante de carbonatos, tanto en entornos palustre-fluvial-lacustres como en lacustres. En las tres unidades, los rudstones de oncoides y fitoclastos se formaron en canales de aguas someras, con baja sinuosidad y en zonas encharcadas, con extensas zonas palustres tobáceas, con desarrollo de plantas hidrófilas. Por el contrario, las calizas micríticas con ostrácodos y las margas corresponden al depósito de calcita en zonas lacustres de aguas tranquilas y permanentes. Por tanto, el sistema sedimentario evolucionó desde un ambiente aluvial-fluvial dominante hasta un ambiente lacustre. Este hecho, junto con el desarrollo de calcretas en las unidades 1 y 2, indica condiciones más húmedas y posiblemente el paso a un lago cerrado hidrológicamente. La falla de Nigüella funcionó a principios del Jurásico como una falla normal, y durante la compresión del Cenozoico provocó la formación de una cuenca sinclinal mediante buttressing del bloque NE contra la falla. Este contexto condicionó la distribución y extensión de litofacies miocenas a lo largo del espacio y del tiempo y la localización de depocentros. La disminución de la actividad tectónica a lo largo del intervalo estudiado favoreció la incisión fluvial, la captura del acuífero mesozoico y la salida del agua subterránea rica en Ca^{2+} y HCO^{-}_{3}, dando lugar al depósito generalizado de carbonato cálcico y, finalmente, a la expansión del lago.

Palabras clave: Depósitos aluviales; Carbonatos lacustres; toba; sedimentación sintectónica; buttressing; Neógeno.

Introduction

There are a number of small intra-mountain basins developed during the Alpine orogeny in the Iberian Range that are filled with alluvial, fluvial and lacustrine deposits of Paleogene and/or Neogene age (*e.g.*, Vera, 2004) (Fig. 1). Their sedimentary evolution and tectonic context are testimony of the relief and climate evolution, as well as of the hydrological characteristics of the sedimentary systems. In contrast to the Calatayud, Montalbán, Aliaga or Teruel basins (Fig. 1B), which have been the focus of numerous and detailed geological studies (Gabaldón *et al.*, 1991; Sanz Rubio, 1999; Ezquerro, 2017 and references therein), the Palaeogene and/or Neogene outcrops between the Moncayo Massif and the Sierra de Vicort have received little attention from a stratigraphic and tectonic point of view. As a matter of the fact, the only published studies are the geological maps on a 1:50,000 and 1:200,000 scale (Hernández-Samaniego *et al.*, 1972; Aragonés Valls *et al.*, 1978; Ramírez del Pozo *et al.*, 1978; Hernández-Samaniego *et al.*, 1978; Olivé Davó *et al.*, 1983; Robador Moreno *et al.*, 2006).

In this region between the Moncayo Massif and the Sierra de Vicort, the Neogene deposits (age provided by Ramírez del Pozo *et al.*, 1978) consist of conglomerates, sandstones and mudstones formed in alluvial and fluvial systems that were related to carbonate deposits (limestones and marls) that formed in fluvial and lacustrine environments. Limestones include a great variety of sedimentary facies, such as tufa, oncolites and stromatolites, as well as thick bioclastic limestones (Ramírez del Pozo *et al*., 1978; Santos Bueno, 2015). Although tufas are not common in the Pre-Quaternary record, in this region these deposits are thick and well preserved, and therefore represent a significant source of information

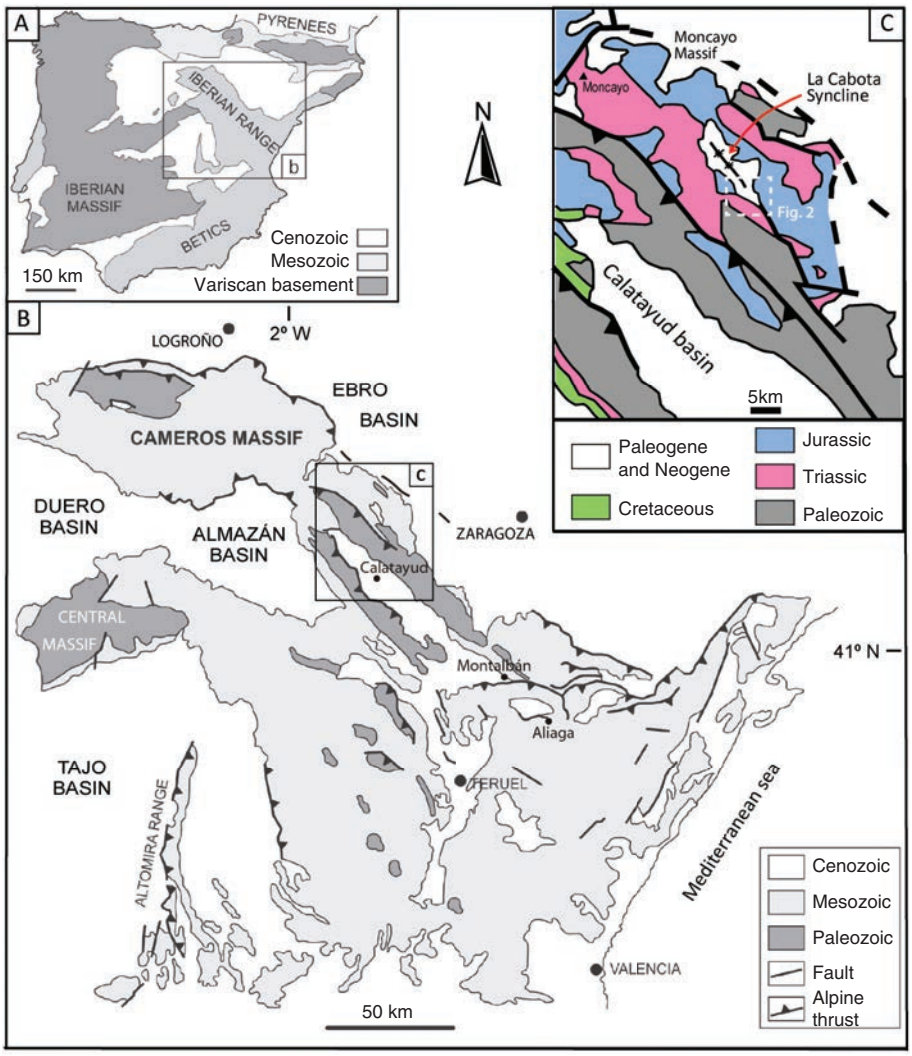

Figure 1.—A) and B) Geological situation of the studied area in the north-western part of the Iberian Range. C) General geology of the studied area, adapted from Sopeña & De Vicente (2004).

concerning climate and drainage arrangement in the past.

Different ductile and brittle deformation structures affecting the Neogene strata suggest a complex tectonic evolution. Actually, the available geologic maps suggest that some pre-Neogene tectonic structures conditioned the deformation style during the Alpine orogeny, influencing the arrangement of sedimentation areas, surface drainage and lithofacies distribution during the Cenozoic.

The aim of this work is to discuss the sedimentary evolution (depositional context and fill geometry) of a small area with Neogene fluvial and lacustrine deposits (Fig. 1C) and its relation to allogenic factors, in particular the effects of Alpine compressional tectonics affecting a major, previously extensional fault. The study demonstrates that the depositional fill context is similar to models for formerly extensional asymmetrical basins (i.e., semi-graben basins), and represents an example of combined tectonics, climate changes and drainage pattern evolution.

Geological setting

The study area is located in the northwestern sector of the Iberian Range, to the south of the Moncayo Massif (Fig. 1A, B), in the southernmost end of a NNW-SSE trending kilometric-scale Cenozoic

syncline, the La Cabota syncline, that folds part of the Cenozoic sequence, as described by Ramírez del Pozo *et al.* (1978) (Figure 1C). In this area, the stratigraphic sequence includes Lower Cambrian and Lower Devonian sandstones and mudstones, Triassic clastic rocks, carbonates and evaporites (Buntsandstein, Muschelkalk and Keuper Facies, and Imón Formation), Jurassic carbonate breccias (Cortes de Tajuña Formation) and evaporites (Lécera Formation), and Cenozoic conglomerates, sandstones, mudstones and limestones (Fig. 2A). These units have been affected by different tectonic

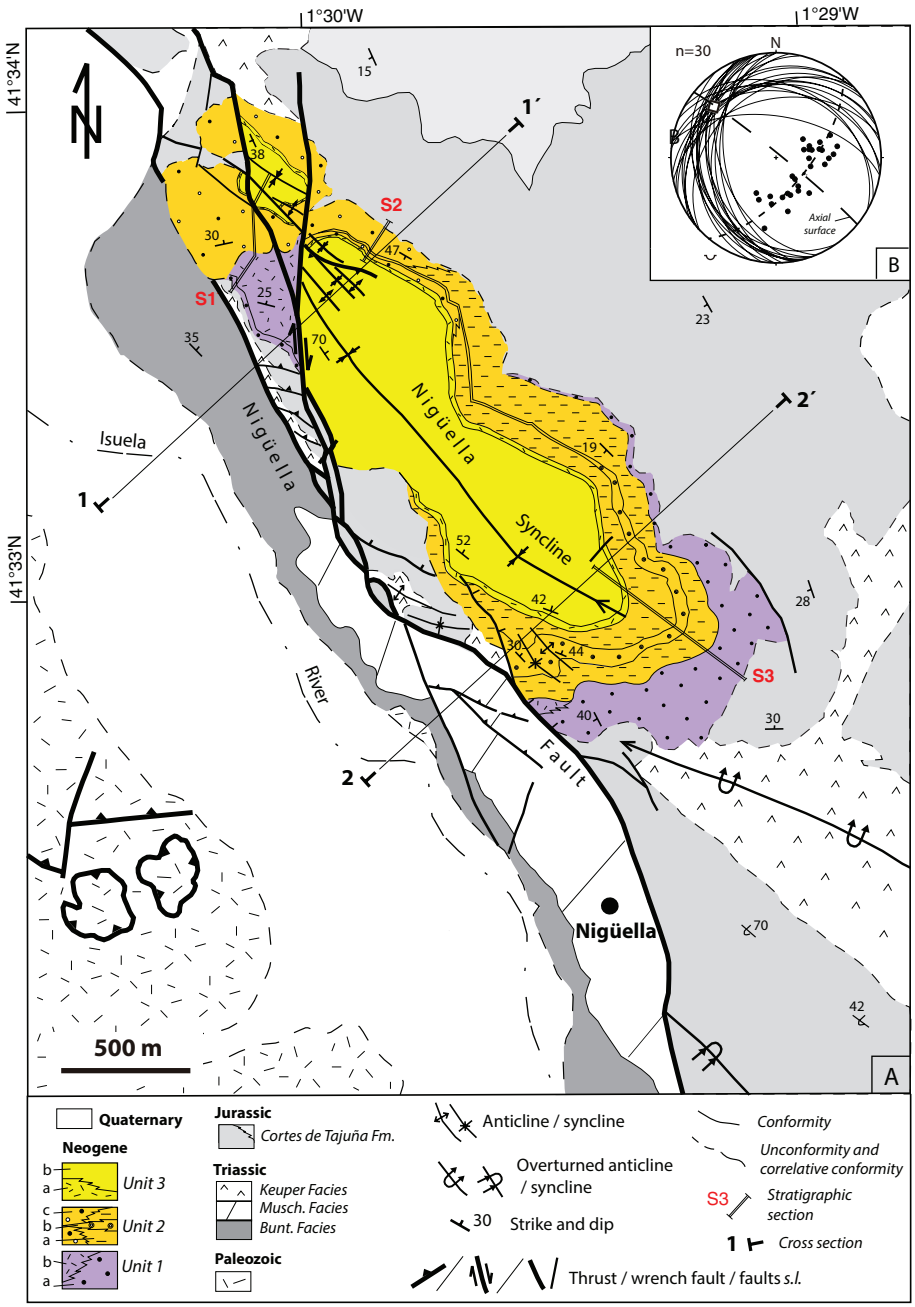

Figure 2.—A) Geological map of the Nigüella studied area. B) Stereoplot (equal area projection, lower hemisphere) of bedding planes (great circles and poles) of Cenozoic units throughout the Nigüella syncline. Movement plane (dashed line) and regional folding axis (white square) are also shown.

phases during the Hercinian and Alpine orogenies. The Mesozoic and Cenozoic sequence has been affected by a dominant NW-SE trending folding and fracturing, which are disharmonic in relation to the Paleozoic basement.

The Cenozoic rocks lie unconformably on pre-Cenozoic rocks. The total thickness is approximately 350 m. Two units are differentiated: 1) conglomerates, mudstones and rare sandstones with interbedded limestones and marls, of Burdigalian-Upper Vindobonian and Pontian age, at the lower part, and 2) limestones (oncolitic limestones, micritic and pelmicritic limestones) and marls of Upper Vindobonian-Pontian age, at the upper part. These ages are based on the presence of *Cypria curvata* LEN., *Hydrobia* and *Limnaea* (Ramírez del Pozo *et al*., 1978). The studied area comprises a small extent to the north of the locality of Nigüella (Fig. 2A). Despite the age uncertainly of these fossils, in this work it is considered that the studied record is of Miocene age, given the lack of other dating criteria at this moment.

Material and Methods

A detailed geological mapping at 1/10,000 scale was made to determine the spatial distribution of the studied Miocene sequence, in the southern part of the La Cabota syncline (Figs. 1C and 2). Three stratigraphic sections that cover the full Neogene record were measured and correlated based on cartographic, lithologic and textural criteria. Indeed, the continuity of beds in the field allowed to know the spacial distribution of the several lithological units that compose the Miocene record. A total of thirty nine rock samples were taken. Fifteen polished sections and twenty thin sections of different facies were studied with a binocular microscope and a petrographic microscope for textural and structural characterization. In addition, five samples were studied in Scanning Electron Microscope of the University of Zaragoza (Carl Zeiss MERLIN™ FESEM). Nomenclature used for detrital facies follows Miall (1978, 2006)'s code and for carbonate rocks is based on Vázquez Urbez (2008) and Arenas-Abad *et al*. (2010)'s code. Texture of carbonate rocks follows classification by Dunham (1962), with modifications by Embry & Klovan (1971), and in the case of sandstones the Pettijohn *et al*. (1973) classification. The structural study included both a structural analysis from field data, coming from bedding planes and hinge lines, and several detailed geological cross sections in order to characterize the structural geometry at a regional scale and visualize the tectosedimentary relationships.

The structure of the Nigüella sector

The Miocene studied units unconformably lie on both Triassic and lower Jurassic strata (Figs. 2A, 3, 4). The dominant NNW-SSE Alpine structural trend in the studied area is characterized by two kilometric-scale structures: 1) the Nigüella fault, and 2) the Nigüella syncline, subparallel to this fault (Fig. 2A). The fault put into contact Triassic rocks, in the footwall, with Cenozoic rocks, in the hanging-wall (Fig. 2A, 3). Towards its northern edge, this fault changes to a N-S trend with dominant dextral-normal component (Figs. 2A, 3A). As shown by cross section in figure 3A, the lower Jurassic strata are involved in a large horse in the vicinity of this sector. The Nigüella syncline, involving different Miocene units, runs with a mean axis orientation 26, 306 and an axial surface orientation 128,84N (Fig. 2B), with dips ranging between 19°, in its central part, up to 70°, in its northwestern part (Figs. 2, 3). Two other NW-SE trending southwest-vergent folds, affecting upper Triassic and lower Jurassic strata, represent the southern prolongation of the Nigüella syncline (Fig. 2A).

Stratigraphy

In the southernmost end of the La Cabota syncline (Fig. 1C), where the study area is located (Nigüella syncline in figure 2A), the Miocene succession varies, from north to south, from 77 m to 120 m in thickness. The stratigraphic sections measured in the studied Miocene sequence (S1, S2 and S3) allowed to distinguish three stratigraphic genetic units that have been correlated based on cartographic and stratigraphic criteria (*i.e.*, the sedimentary evolution of the sequences and the presence of sharp lithological changes). Units 1 and 2 are separated through an angular unconformity in the north and a correlative conformity towards the south. In contrast, the boundary between units 2 and 3 is a sharp lithological change throughout the studied area (Figs. 2A and 5).

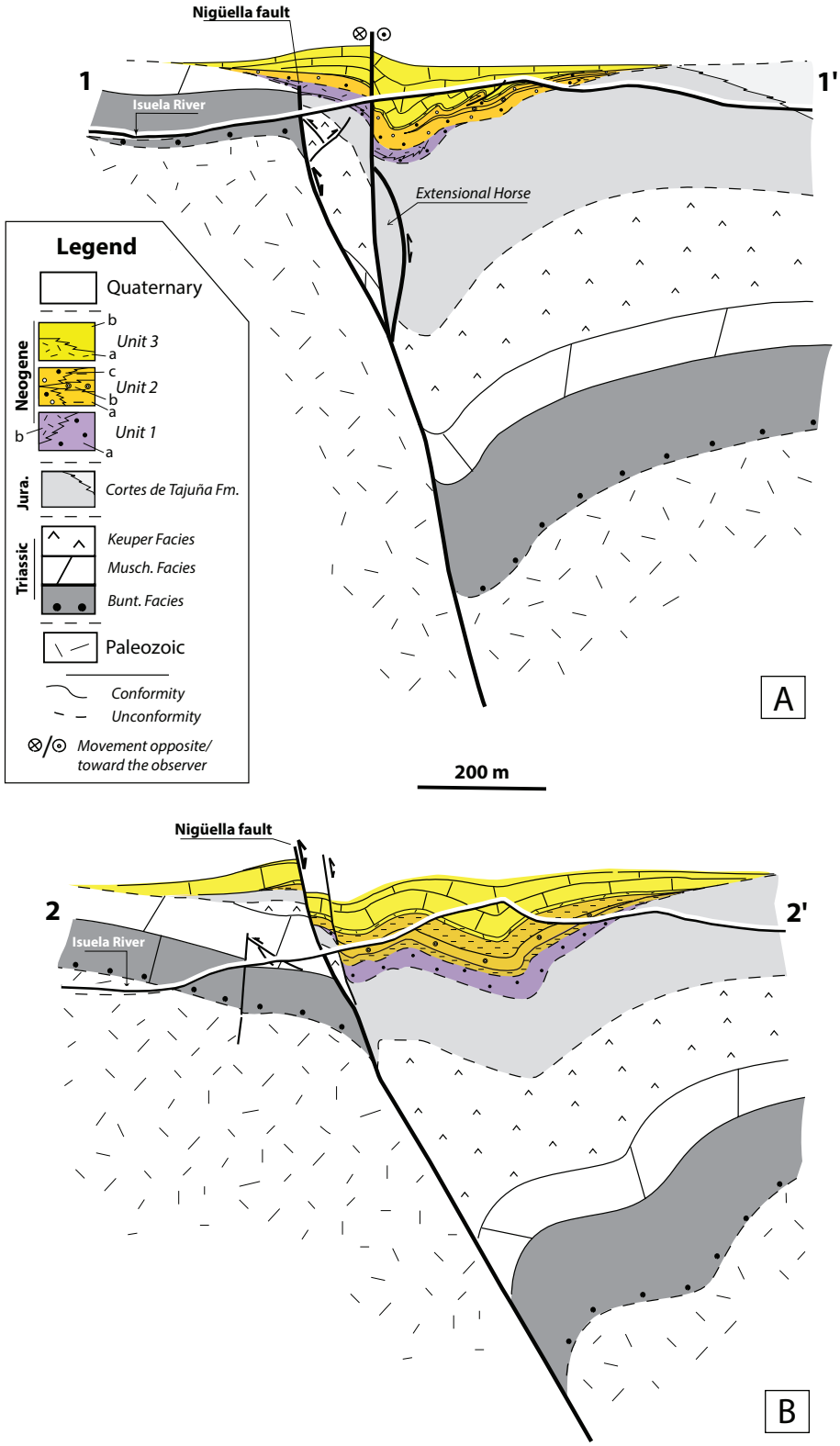

Figure 3.—Geological cross sections of the studied area (location in Figure 2).

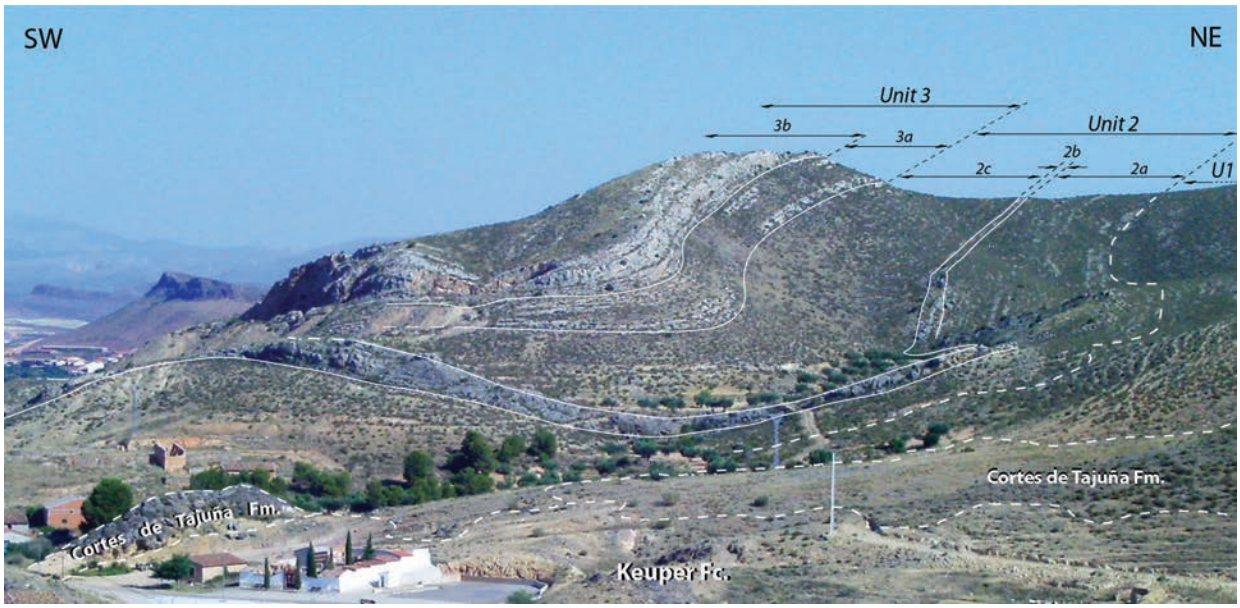

Figure 4.—Panoramic view of the Niguella's syncline on its southern part. The different stratigraphic units are differentiated with dash and continuous lines, corresponding to unconformable or geometrically parallel contacts (likely conformities), respectively.

Unit 1 crops out to the west and south of the studied area. It lies unconformably on the Upper Triassic and Lower Jurassic rocks. The boundary with Unit 2 is an angular unconformity in the west (*e.g.*, section 1) and a correlative conformity in the south (*e.g.*, section 3). The vertical sedimentary evolution is fining upward. In section 1, this unit is formed of 29 m of monomict grey conglomerates at the base, mostly consisting of carbonate clasts from upper Triassic and Jurassic rocks and also phytoclasts and oncoids among the clasts, followed by phytoclast and oncoid packstones and rudstones, and then bioclast and oncoid wackestones. In section 3, Unit 1 consists of monomict grey and light brown conglomerates and ochre, orange and red mudstones, with rare interbedded grey limestones. This unit encompasses calcretes. The monomict conglomerates are formed primarily of carbonate Upper Triassic and Jurassic-derived carbonate clasts, varying from rounded to angular in shape.

Unit 2 crops out throughout the studied area. It lies on the Mesozoic substrate in the northeast (*e.g.*, section 2) and on Unit 1 in the rest of the study area. The upper boundary with Unit 3 is a sharp lithological change, *i.e.* from clastic deposits to dominant limestones. The evolution of Unit 2 is cyclic, fining and then coarsening upward. In section 1, Unit 2 is 62 m thick and is formed of polymict conglomerates, consisting of clasts formed of Jurassic limestones, Triassic sandstones, dolostones and limestones, and Paleozoic-derived sandstones and quaztarenites, up to 0.9 m long. The unit also includes rare mudstones and phytoclast limestone interbeds. In section 2, Unit 2 is 47 m thick and the outcroping portions show mostly conglomerates and minor phytoclast limestones. In section 3, Unit 2 is ≈ 50 m thick and includes monomict and polymict conglomerates that alternate with ochre and orange mudstones, marls and minor phytoclast, oncoid and bioclast limestones.

Unit 3 crops out throughout the study area and consists of two differentiated portions. The lower one with phytoclastic and oncolitic limestones, 25 to 35 m thick, and the upper one with fine-grained bioclastic, micritic limestones with variable presence of marly interbeds, up to 16 m thick. The total thickness of this unit increases southward, from 30 m in sections 1 and 2, to 45 m in section 3 (Fig. 5).

Sedimentology

Diverse clastic (allochtonous sediment) and carbonate (authochtonous sediment) lithofacies are distinguished based on lithology, texture, microstructure and nature of components. Table 1 shows the

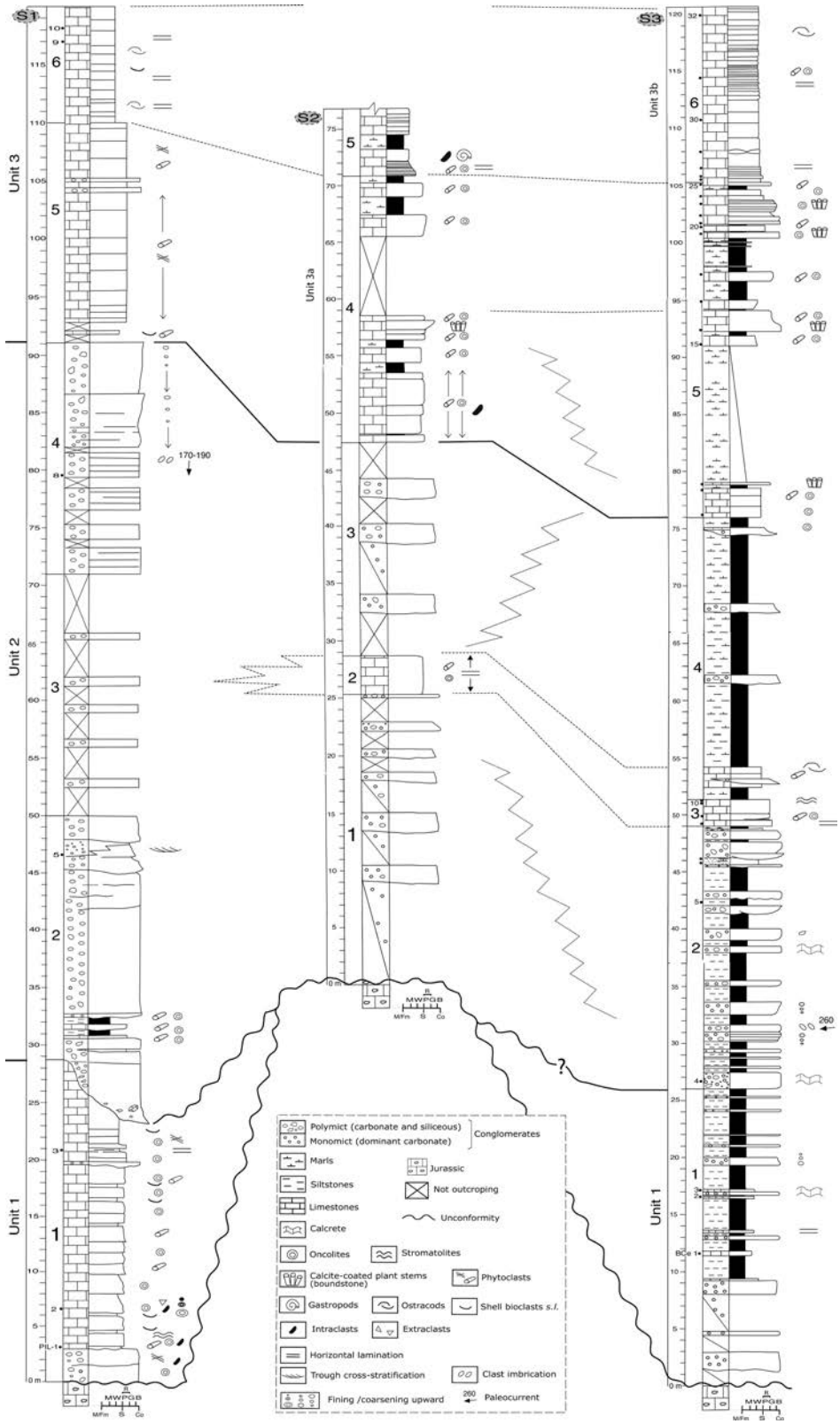

Figure 5.—Stratigraphic sections measured in the studies area and their correlation based on cartographic, lithologic and textural criteria. S1: La Pilona section. S2: Los Bancales section. S3: Cementerio section. Location is in figure 2.

Table 1.—Lithofacies and their characteristics in the studied area. Lithofacies Nomenclature and abreviations adapted to the study case from Miall (1978)'s code and Arenas-Abad et al. (2010)'s code. Facies associations (FA) are those represented in figure 8.

Lithology (Figures)	Texture and geometry of deposits	Sedimentary Facies and facies associations (FA)	Interpretation: processes and depositional settings
Conglomerates (Fig. 6A to F)	Monomict, mostly carbonate clasts: Gm1, Gh1 Grey in colour. Clast-supported fabric. Most clasts of dark grey limestones and dolostones from Upper Triassic and Jurassic carbonates. Minor and smaller clasts of brownish to reddish sandstones from Lower Triassic and Paleozoic rocks. Commonly heterometric, from a few cm to 32 cm long; varied in shape and from subangular to subrounded. Very coarse sand and granule matrix, and calcareous cement. Calcretized at many places. Generally thick, up to 1.5 m, tabular bodies with crude stratification, and planar or wide concave bases. Polymict: Gm2, Gm3, Gh2, Gt2 Grey to light brown in colour. Clast-supported fabric. Clasts of grey and light brown limestones and dolostones and reddish sandstones from Triassic and Jurassic rocks, and of light brown, grey and reddish sandstones and dolostones from Paleozoic rocks; at places tufa-derived intraclasts are also present (Gm3). Commonly heterometric, from a few cm to 100 cm long; varied in shape and from poorly rounded to rounded. Very coarse to medium sand and granule matrix of the same composition and minor calcareous cement. Locally, calcretized. Generally thick, up to 2.5 m, tabular bodies with crude stratification, and planar or wide concave bases. Locally, wedge- and lense-shaped bodies up to 1 m thick.	**Gm1, Gm2**: structureless, without clast-size vertical trend. Fig. 6A	Flash flood deposits in proximal sectors of alluvial fans and bar cores in braided fluvial context (Miall, 1978, 1996; Arenas *et al.*, 1989)
		Gm1a, Gm2a: fining-upward trend. FA A2, A3. (Fig. 6F)	Deposition from slightly channelled and sheet-shaped high-velocity expanding flow that then waned (Ashley, 2002; Kumar *et al*., 2007).
		Gm1b: coarsening-upward trend. FA A2. (Fig. 6B).	Gravel lobes in proximal sectors of alluvial fans (López-Gómez & Arche, 1997; Kumar *et al*., 2007).
		Gm1c, Gm2c: with imbricated clasts. FA A1, B. (Fig. 6C, D)	Gm1c, Gh1: Deposition from a high-velocity flow in proximal-middle sectors of alluvial fans (Fielding *et al*., 2007; Shukla, 2009).
		Gh1, Gh2: horizontal stratification, with or without clast imbrication. FA B.	Gm2c, Gh2: Deposition in longitudinal bars of braided fluvial systems (Miall, 1978, 2006).
		Gt2: through cross-stratification, sets dm thick. FA B.	Deposition in transverse bars and crescent dunes in shallow braided channels (Miall, 1978, 2006; Fielding *et al*., 2007).
		Gm3: structuress, commonly fining-upward. FA C.	Gm3: Distal fluvial, gently channelled flows that transport small-size polygenic extraclasts along with intraclasts, mostly tufa-derived particles.
Sandstones (associated with polymict conglomerates) (Fig. 6E, F)	Grey and light brown litoarenites. Very coarse sand size. Poorly rounded to subrounded grains (quartz and limestone); with calcareous cement. Generally tabular, with planar or slightly concave bases, and locally lenticular (channel-like). Internal concave surfaces. Up to 1 m thick.	**Sm:** structureless or with fining-upward trend. FA B.	Deposition from a high-velocity expanding flow in alluvial plains (Ashley, 2002).
		St: trough cross-stratification, sets dm thick. FA B.	Deposition in shallow braided fluvial systems, frequently as channel fills (St<=> Gt2) (Miall, 1978; Allen, 1982a, b).
Siltstones and silts: Fines. (Fig. 6B, E, F)	Reddish, yellowish and light brown silt-size siliciclastics. Tabular strata, 0.05 to 2 m thick, in some cases grouped into sets up to 4 m thick.	**Fm:** structureless. FA A1, A2, A3, B.	Fine detrital deposition in inactive alluvial and fluvial areas, e.g. floodplain (Arenas & Pardo, 1999; Porter & Gallois, 2008).
Marlstones and marls. (Fig. 6G, I)	Yellowish to beige lime mud and clays or silt-size siliciclastics. In some cases, including mm to sub-mm silt laminae. Tabular strata up to 2 m thick.	**M**: structureless. Disperse molluscs and phytoclasts. FA D1, D2.	Settle out of fine siliciclastics (from alluvial supply) and lime mud in shallow, mostly offshore lake areas (Armenteros *et al*., 1997; Arenas & Pardo, 1999).

Continued

Table 1.—Continued

Lithology (Figures)	Texture and geometry of deposits	Sedimentary Facies and facies associations (FA)	Interpretation: processes and depositional settings
Limestones Figs. 6G-M, 7.	Micritic limestones: Light grey, beige and whitish mudstones to wackestones, with or without allochemical components (bioclasts: gastropods and ostracods; phytoclasts and microbial filaments). Tabular strata cm to 2 m thick.	**Lm, Lb**: structureless mudstones (Lm) and wackestones (Lb). Though rare, weak bioturbation (root traces). FA C, D1, D2. (Fig. 6H). **Lh:** mainly mudstones with horizontal lamination. FA D1, D2. (Fig. 6H). **Lp:** mudstones with palustrine features, mostly bioturbation. FA A2.	Lime mud deposition in shallow, still lake areas inhabited by diverse organisms (i.e., ostracods and gastropods) (Platt, 1989; Gierlowski-Kordesch, 2010). Lime mud deposition in offshore, still lake areas (Vázquez-Urbez *et al.*, 2013). Lime mud deposition in very shallow lakes with hydrophilous plants. Subaerial exposure (Platt, 1989; Sacristán-Horcajada *et al.,* 2016).
	Phytoherm limestones: Grey and ochre boundstones consisting of up-growing vertical, in situ, calcite-coated plant stems (external and internal moulds), up to 19 cm high. The coatings are formed of alternating micritic and microsparitic laminae, commonly with microbial evidence. Tabular and lenticular layers 0.15 to 0.40 m thick, commonly as patches or part of strata made of other dominant facies).	**Lst:** boundstones of up-growing calcite-coated plant stems (e.g., reeds, bulrushes, and other hydrophilous plants). FA D1. (Fig. 6I, J).	Calcite precipitation around the submerged parts of hydrophilous plants, commonly with stromatolite structure, in shallow ponds, lake shores and fluvial areas (Vázquez Urbez, 2008; Pedley, 2009).
	Phytoclastic and oncolitic limestones: Grey, ochre and light brown rudstones with matrix, in some cases packstones, formed of oncoids and phytoclasts, 0.2 mm wide and up to 10 cm long. Smaller mm-long grains form fine phutoclastic limestones (Lphf) The nuclei is formed of plant moulds, gastropods, intraclasts and, less commonly, extraclasts. The coatings, up to 2 cm thick, are laminated with abundant microbial evidence. If oncoids dominate, Lo. Tabular and lenticular layers and strata, 0,21 to 2.40 m thick. The thinner form part of strata made of other facies.	**Lph:** calcite-coated phytoclast and less abundant oncoid rudstones and packstones. FA A3, C, D1, D2. (Fig. 6G, K, M; 7C, D). **Lo:** oncoid rudstones and packstones. FA A3, C, D1. (Fig. 6L).	Breakage of hydrophilous plants (with and without calcite coatings) and deposition of phytoclasts and oncoids in nearby slow-flowing fluvial and lacustrine areas (Ordóñez & García del Cura, 1983; Zamarreño *et al*., 1997; Vázquez Urbez, 2008; Pedley, 2009).
	Stromatolites: Light grey and brown, undulate layers, of small lateral continuity, up to 0.3 m thick, commonly patches within facies Lph. Filamentous microbes (micrite filaments and tubes, likely of cyanobacteria and small algae).	**Ls:** stromatolites. FA C. (Fig. 7 A, B).	Calcification of microbial mats in shallow fluvial and lacustrine areas (Riding, 1991a, b; Arp *et al*., 2001).
Calcretes: **Cc**. Fig. 6A.	White and beige, powderly and hard deposits. Very irregular masses, laminated undercoatings and in somes cases layers 0.03 to 0.1 m thick, within conglomerates.		Calcite precipitation within alluvial deposits exposed to prolongued arid conditions (Wright & Tucker, 1991; Alonso-Zarza, 2003).

main characteristics and sedimentological interpretation of the different facies and includes references to works that deal with similar facies and depositional environments. Coarse clastic facies consist of monomict and polymict, clast-supported conglomerates that deposited by dominant aqueous processes. Monomict conglomerates (noted as Gm1 and Gh1) consist of dominant carbonate clasts (dolostones and limestones) derived from Upper Triassic and Jurassic rocks, with less abundant siliceous clasts (sandstones, quaztites and rare siltstones) from Lower Triassic and Permian rocks (Fig. 6A, B). Polymict conglomerates (noted as Gm2 and Gt2) are formed of mixed carbonate and siliceous clasts from Paleozoic

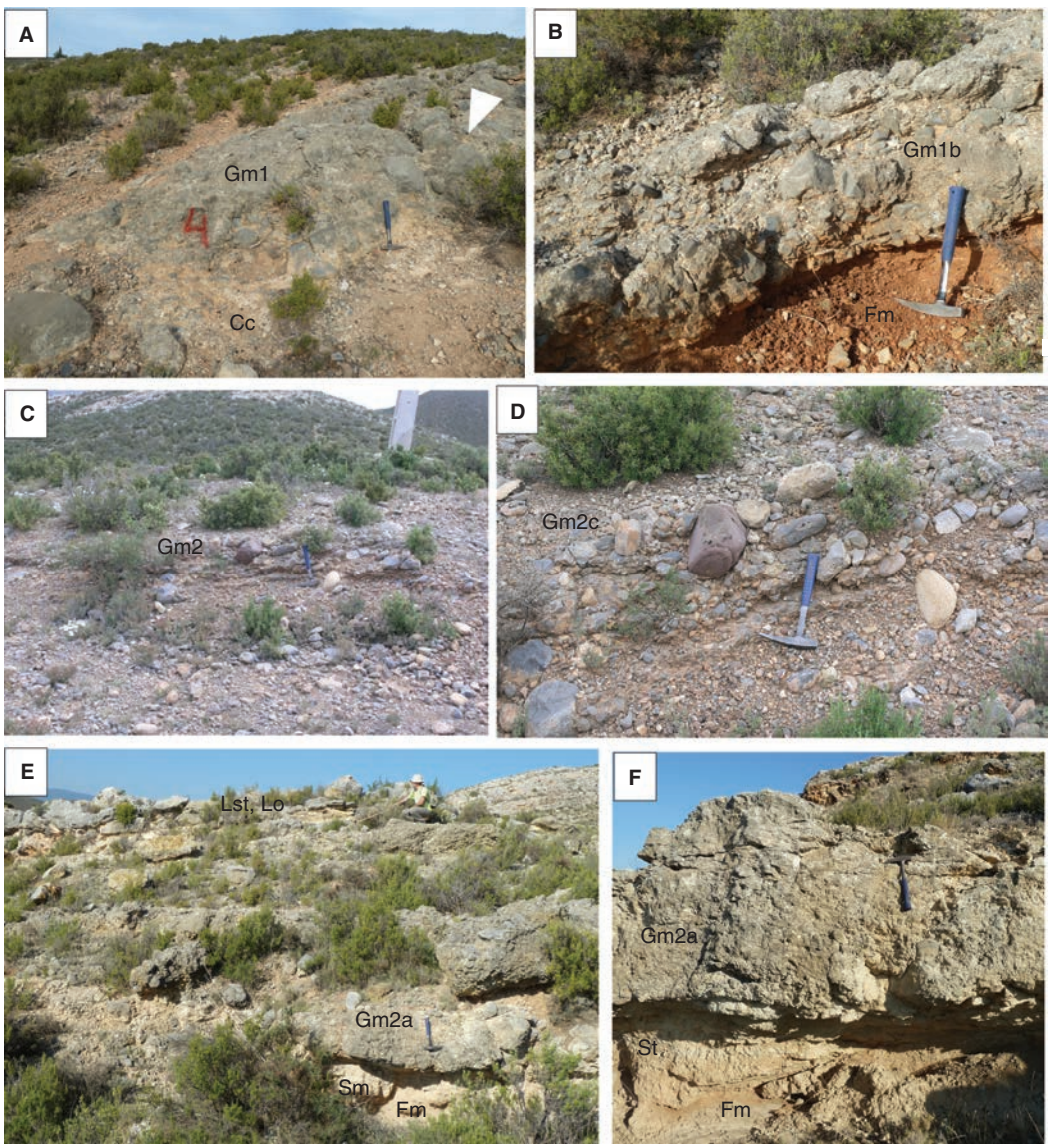

Figure 6.—Field and hand-sample views of sedimentary facies. A, B) Monomict conglomerates formed of carbonate clasts derived from Upper Triassic and Jurassic rocks. Arrow points to a boulder. Note the presence of calcretes in A (Cc) and siliciclastic red mudstones in B. Images from section S3. C, D) Polymict conglomerates with imbricated clasts. Images from section S1. E, F) Polymict Conglomerates with subrounded clasts. Note the slightly channelled conglomerate bases in E and presence of mudstones and sandstones below the coarse-grained deposits in E and F. G) Phytoclast and oncolitic (Lph, Lphf and Lo). Note the presence of Marls (M) and the channelled-shaped surface. H) Micritic limestones with horizontal lamination (Lh). I, J) Boundstone consisting of up-growing calcite-coated stems. K) Laminated coating around a stem (decayed), corresponding to a coated phytoclast. L) Oncoid. M) Detail of phytoclastic limestones.

(*Continued*)

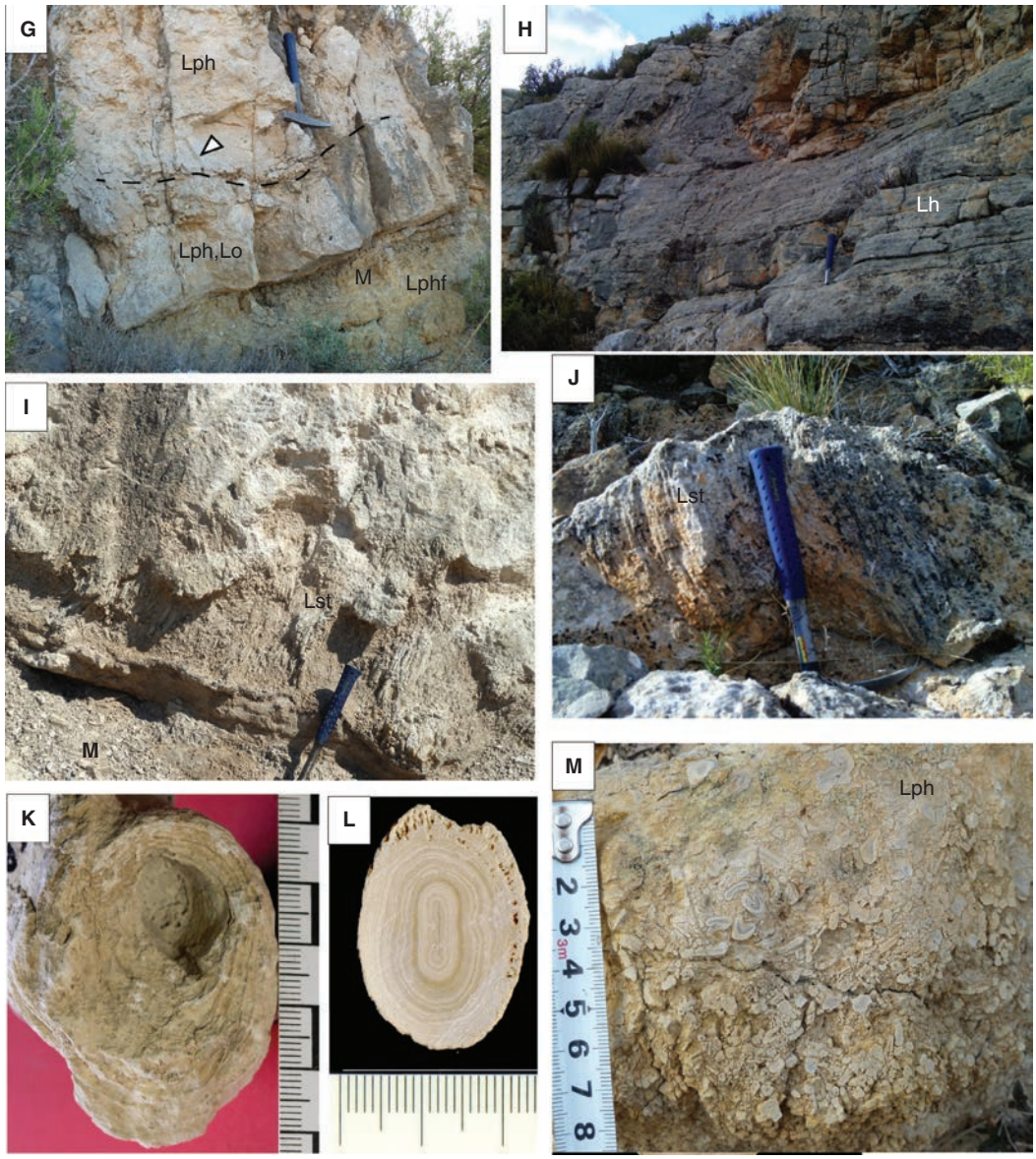

Figure 6 (*Continued*).— Field and hand-sample views of sedimentary facies. A, B) Monomict conglomerates formed of carbonate clasts derived from Upper Triassic and Jurassic rocks. Arrow points to a boulder. Note the presence of calcretes in A (Cc) and siliciclastic red mudstones in B. Images from section S3. C, D) Polymict conglomerates with imbricated clasts. Images from section S1. E, F) Polymict Conglomerates with subrounded clasts. Note the slightly channelled conglomerate bases in E and presence of mudstones and sandstones below the coarse-grained deposits in E and F. G) Phytoclast and oncolitic (Lph, Lphf and Lo). Note the presence of Marls (M) and the channelled-shaped surface. H) Micritic limestones with horizontal lamination (Lh). I, J) Boundstone consisting of up-growing calcite-coated stems. K) Laminated coating around a stem (decayed), corresponding to a coated phytoclast. L) Oncoid. M) Detail of phytoclastic limestones.

and Mesozoic rocks (Cambrian, Permian, Triassic and Jurassic)(Fig. 6C, D). Polymict conglomerates that include intraclasts (mainly tufa-derived clasts) are named Gm3. Textural features along with sedimentary structures of the coarse-grained sediments allow to distinguish:

1) Conglomerates formed of subangular to subrounded clasts, with fining-upward (Gm1a, Gm2a), coarsening-upward (Gm1b, Gm2b) or without clear upward evolution (Gm1, Gm2), that deposited from high energy flows in proximal sectors of alluvial fans (Fig. 6A to

D), probably from dominant sheet flows (*cf.*, Arenas *et al*., 1989; Miall, 1996; López-Gómez & Arche, 1997; Kumar *et al*., 2007).

2) Conglomerates consisting of dominant subrounded clasts (Gh1, Gt2, Gm3; Fig. 6E, F) that deposited in shallow channels and longitudinal and crescent-shape bars of middle and middle-distal sectors of alluvial and fluvial systems (*cf.* Arenas *et al*., 1989; Miall, 2006; Fielding *et al*., 2007; Shukla, 2009).
3) Conglomerates with imbricated clasts, both monomict and polymict (Gm1c, Gm2c), that developed during high-energy floods and also at the top of longitudinal bars, respectively (Fig. 6D) (Fielding *et al*., 2007; Shukla, 2009).

Sandstones are formed of siliceous and carbonate grains. They are rare and form lenticular bodies up to 1 m thick, either structureless (Sm) or with trough cross-stratification (St), always associated with facies Gt2 (Fig. 6E, F). Siliciclastic mudstones (Fm), which associate with the conglomerates (Fig. 6B, E, F), resulted from fine-size sediment deposition during flooding on inactive sectors of the alluvial and fluvial systems (*i.e.*, floodplains) (Porter & Gallois, 2008).

Carbonate facies are varied (Fig. 6G to M). Three groups are present:

1) Tufa and microbialitic facies: Phytoherm limestones consisting of up-growing calcite-coated stems (Lst, Fig. 6I, J) that formed by calcite precipitation around the submerged parts of hydrophilous plants (Pedley, 1990; Vázquez-Urbez, 2008). Breakage of these calcite-coated plants and other non-coated plants produced fragments that eventually gave rise to phytoclastic limestones (Lph; Fig. 6M). Some fragments could become the nuclei for oncoids. In general, phytoclasts and oncoids appear mixed in facies Lph, but oncoids may be the dominant component in some limestones (Lo; Fig. 6K, L). In both cases, the calcite coatings are laminated and encompass microbial components (*i.e.*, they are stromatolitic structures; Fig. 7A to D). Facies Lph, Lo and Lst (Fig. 7 C, E) are associated with each other and formed in shallow ponds, lakeshores and stream areas, in which water would be over saturated in calcite (Ordóñez & García del Cura, 1983; Zamarreño *et al*., 1997; Pentecost, 2005; Pedley, 2009; Arenas-Abad *et al.*, 2010). Stromatolites (Ls) are not abundant; they form thin and discontinuous deposits over or between the phytoherm limestones (Fig. 7A, B, D); they represent calcification of microbial mats consisting of filamentous cyanobacteria (Fig. 7A, B; *cf.* Riding, 1991a, b) in shallow lacustrine and fluvial areas (Arp *et al.*, 2001; Vázquez-Urbez, 2008; Arenas-Abad *et al.*, 2010).
2) Fine-grained limestones: Micritic limestones (Lm) can form tabular, at places thick, strata (up to 2.8 m, Fig. 6H) formed of mudstones and mudstones-wackestones consisting mainly of ostracods, rare gastropods and microbial filaments (Figs. 7F, G, H). These limestones show horizontal lamination and rare weak vertical bioturbation. They formed in still and permanent water areas inhabited by diverse freshwater biota (*cf.*, Platt, 1989; Gierlowski-Kordesch, 2010; Vázquez-Urbez *et al.*, 2013). Marls (M) associated with limestones formed by settling out of fine siliciclastics and lime mud on lake floors, mostly offshore, in dominantly calm conditions (Armenteros *et al.*, 1997; Cabrera *et al*., 2002). In general, they are associated with water inputs that carried fine siliciclastic sediment into the lake (*e.g.*, Arenas & Pardo, 1999).
3) Calcretes: These include laminar structures, hard irregular masses, and mostly clasts with laminated coatings, which developed in the conglomerates, limestones and siliciclastic mudstones that formed in proximal alluvial fans (Fig. 6A). They represent interruptions in alluvial and lacustrine sediment accretion that occurred during arid periods (*e.g.*, Alonso-Zarza, 2003; Alonso-Zarza & Arenas, 2004; Sacristán-Horcajada *et al*., 2016).

Facies associations

The different facies are associated vertically into simple sequences (*i.e.*, facies associations, FA) that represent cycles of variation of water level and/or flow conditions (*e.g.*, hydrodynamics), and the

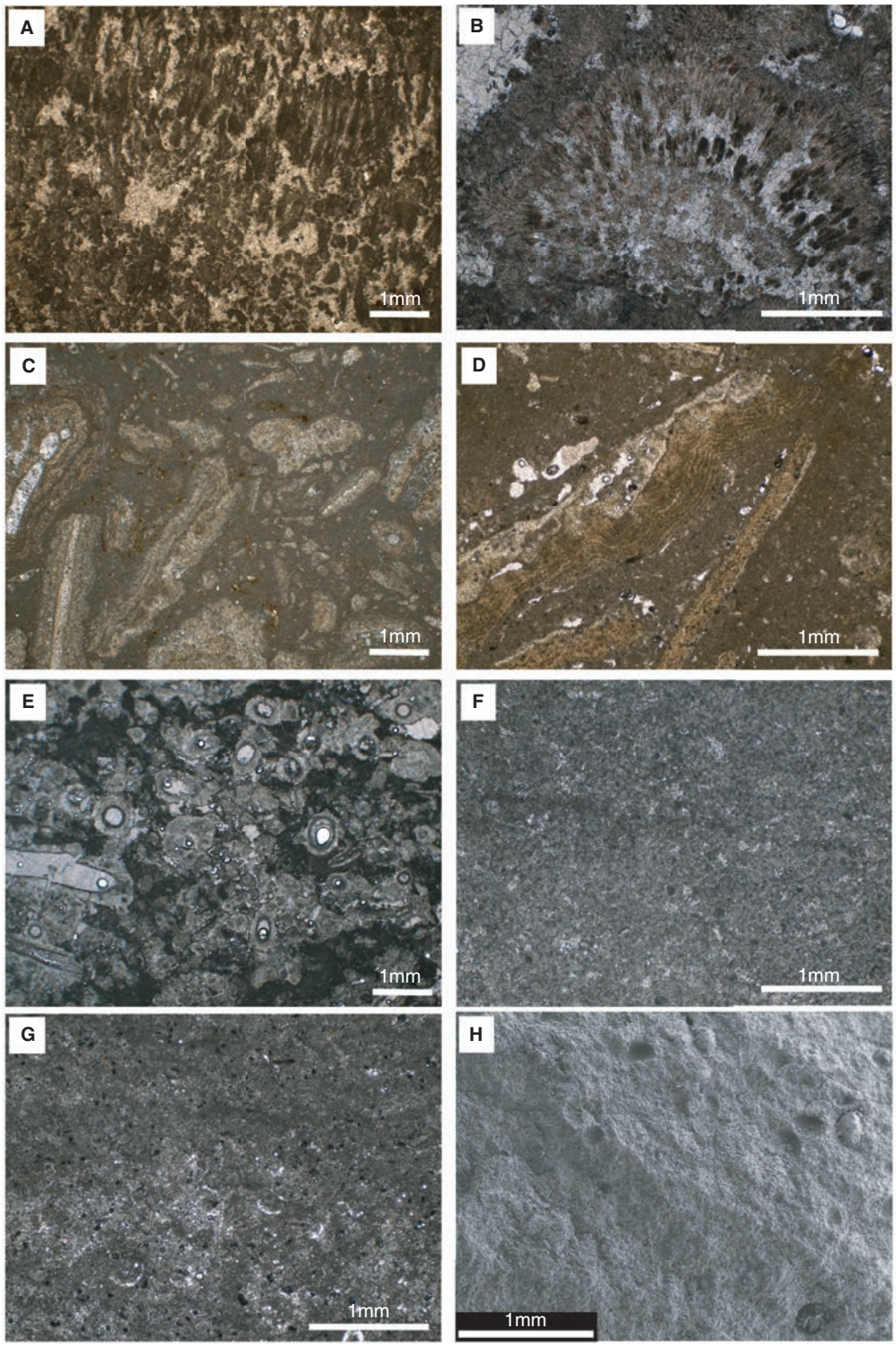

Figure 7.—Photomicrographs of sedimentary facies (A-G, optical microscope; H, Scanning Electron Microscope). A, B) Stromatolites. C, D) Phytoclastic limestone. Note laminated calcite in a stromatolite fragment. E) Phytoclastic limestone with coated stems in cross and longitudinal sections. F, G, H) Micritic limestones with ostracods, microbial filaments and dark stem fragments. Note in F and H, subtle lamination. Ovoid and sub-spherical cavities in H probably correspond to ostracods.

migration of active parts of the fluvial system (*e.g.*, by channel fill) as a result of progradation, retrogradation or lateral accretion processes. Seven main FA have been recognized (Fig. 8). Three FA correspond to deposition in proximal and middle areas of alluvial fans (FA A1, A2 and A3). These FA have been observed in the southern and northern studied areas. FA A1 formed as a result of flash floods that deposited coarse gravel (facies Gm1) in the form of lobes over floodplain areas with fines (facies Fm) producing "blankets"; the progradation of gravel sheets or lobes produced coarsening upward evolution and crude horizontal stratification (Arenas, 1993; López-Gómez & Arche, 1997). In contrast, FA A2 represents gravel deposition from gently channelled and sheet flows that were filled with poorly sorted and disorganized gravels. Then, these channels quickly waned up to become inactive areas with episodic deposition of facies Fm. Similar associations have been described in the upper Permian of the Iberian Ranges (López-Gómez & Arche, 1997) and the Middle Miocene of the Ebro Basin (Vázquez-Urbez *et al.*, 2013). Shallow lakes could develop in these inactive areas, and be sites for lime mud deposition (facies Lp at the top of FA A2). These carbonate deposits could develop in middle-distal alluvial areas and in inactive areas between alluvial fans (Platt, 1989; Sacristán-Horcajada *et al*., 2016). In both alluvial fan FA A1 and A2, dry conditions would have allowed the development of calcretes during the cease of alluvial accretion (Wright & Tucker, 1991; Alonso-Zarza, 2003; Sacristán-Horcajada *et al.*, 2016).

FA A3 formed by coarse polymict gravel deposition in gently channelled and sheet flows that quickly waned in proximal and middle alluvial sectors, then becoming sites for fine deposition (facies Fm). Oncoid and phytoclast facies that follow up in the sequence give evidence of shallow carbonate fluvial deposition. This type of carbonate deposition on top of coarse gravel deposits is common in Quaternary fluvial systems of the Iberian Range (Vázquez-Urbez *et al.*, 2012). The incomplete FA

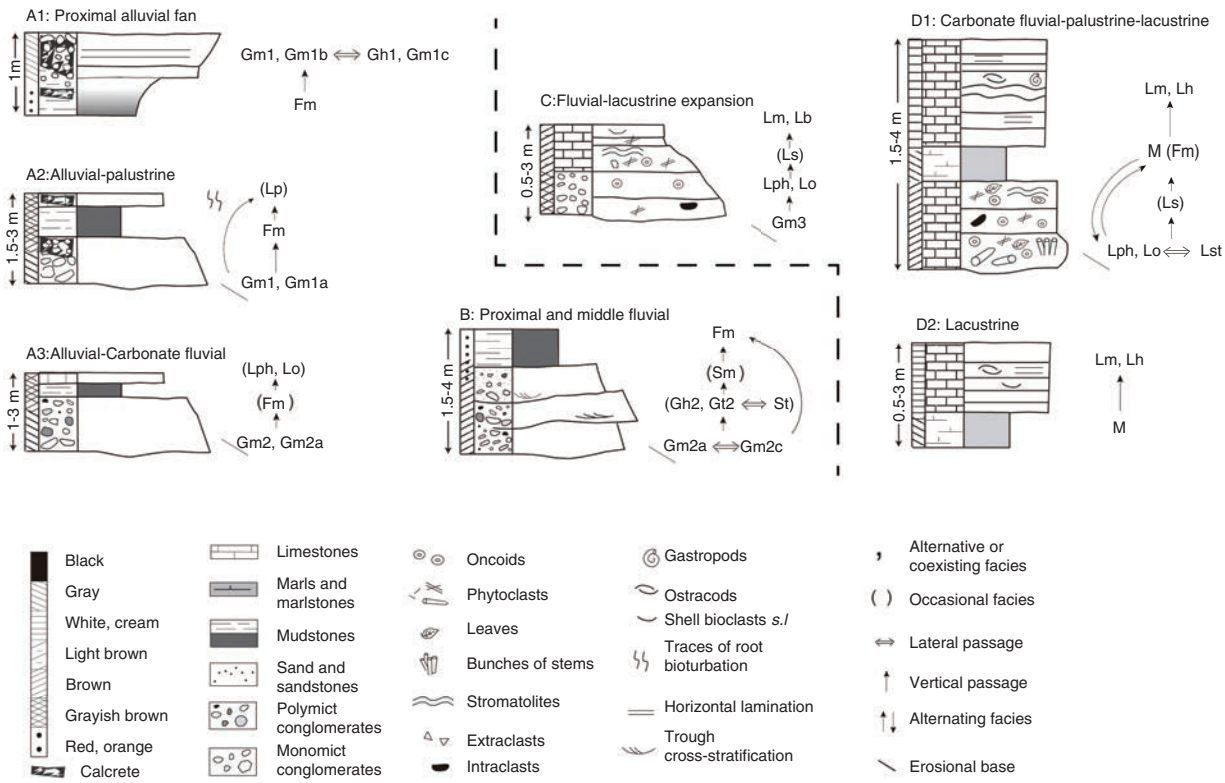

Figure 8.—Vertical facies association (FA). Explanation in the text. The line separates dominant carbonate fluvial and lacustrine associations from clastic alluvial and fluvial associations (extraclasts).

A3, lacking the carbonate part, is common in Unit 2 in the northern studied area.

FA B is a fluvial association that formed by polymict gravel and rare sand deposition in shallow channels and longitudinal and transverse bars (facies Gm2a, Gm2c, Sm, St) of a braided fluvial system whose floodplain broadened southwards (*i.e.*, with increasing extent of facies Fm in the southern section 3, Fig. 5). Accordingly, the sequence shows varying thickness of fines and changing size and shape of clasts depending on the location through the system. Siliceous and carbonate clasts with moderate to good roundness suggest long and/or energic transport. This FA is common in middle and middle-distal sectors of fluvial systems (Arenas *et al*., 1989; Miall, 2006).

FA C has been defined in the northern and southern studied area. It represents fine-size gravel deposition channels of distal sectors of a fluvial system that included mixed extraclast-intraclast sediment (facies Gm3) and finally was replaced with carbonate deposition in shallow channels (facies Lph, Lo and occasionally Ls). These areas later became site for lime mud deposition in shallow lakes (facies Lm). Therefore, it corresponds to a change from clastic to carbonate deposition with final expansion of standing water bodies. Similar associations have been described in the Oligocene fluvial deposits of Mallorca (Arenas *et al.*, 2007).

Two FA represent dominant carbonate deposition, either lacustrine or palustrine-fluvial-lacustrine (FA D1 and FA D2). The lower part of FA D1 represents formation and deposition of oncoids and phytoclasts (facies Lo, Lph) in shallow, low-sinuosity channels and pools with extensive tufaceous palustrine areas, where hydrophilous plants would be dominant (Lst). The environment would be consistent with a low-gradient fluvio-lacustrine context characterized by having water with high Ca and HCO^-_3 content (*e.g.*, as described by Ordóñez & García del Cura, 1983; Pedley, 1990; Pentecost, 2005; Arenas-Abad *et al*., 2010). This context evolves upwards to marls (M), which represent rapid expansion of lacustrine conditions consequent to increased water inputs. Afterwards extensive lime mud deposition in shallow quiet conditions took place (facies Lm and Lh; *i.e.*, top of FA D1 and D2 in Fig. 8). In brief, FA D1 records the expansion of carbonate lacustrine sedimentation over fluvial and fluvio-lacustrine carbonate settings. Similar sequences have been found in the late fill stage of the Cenozoic Calatayud Basin (Sanz-Rubio, 1999) and Ebro Basin (Arenas *et al*., 2000; Vázquez-Urbez *et al*., 2013). FA D2 corresponds to offshore dominant carbonate lacustrine deposition producing micritic limestones with ostracods that typically occur in still and permanent lakes (*cf*., Platt, 1989; Cabrera *et al*., 2002, 2011; Gierlowski-Kordesch, 2010; Vázquez-Urbez *et al.*, 2013).

Discussion

Sedimentary evolution, paleogeography and structural constraints on sedimentary features

Sedimentological data of the studied Neogene succesion indicate a sedimentary context consisting of alluvial and fluvial environments related to carbonate fluvial-lacustrine-palustrine and lacustrine environments. The occurrence and distribution of such environments through space and time (Fig. 9) and the location of the main depocentre in the study area (*i.e.*, towards the southeast and parallel to the main syncline axial trace; Figs. 2 and 5) were closely related to the local tectonic evolution. A cross section normal to the Nigüella syncline shows that the maximum thickness of the detrital deposits (Units 1 and 2) is found in the vicinity of its hinge zone and the thickness decreases outward the syncline axis (Figs. 2 and 5). This fact suggests a strong tectonic control on the sedimentary thickness and the surface drainage arrangement. Several evolutionary stages have been sketched (Fig. 9).

Depositional Stage 1 (Unit 1) recorded alluvial fan deposition (FAs A1 and A2 in Fig. 8; Fig. 9A) that stemmed from eastern and southeastern close uplands, less commonly from western uplands, which surrounded the study area. Moreover, a distal south-flowing fluvial system occupied part of the northern area, coinciding and finally being replaced with a carbonate fluvial system flowing southeastward. Shallow carbonate lakes developed locally between the carbonate channels (FA C), and beyond the toe of the alluvial fans, mostly on mud-dominated areas (FA A2). Suspended sediments transported beyond the fan toe, along with dissolved ions, could be pooled in shallow areas, where the fine

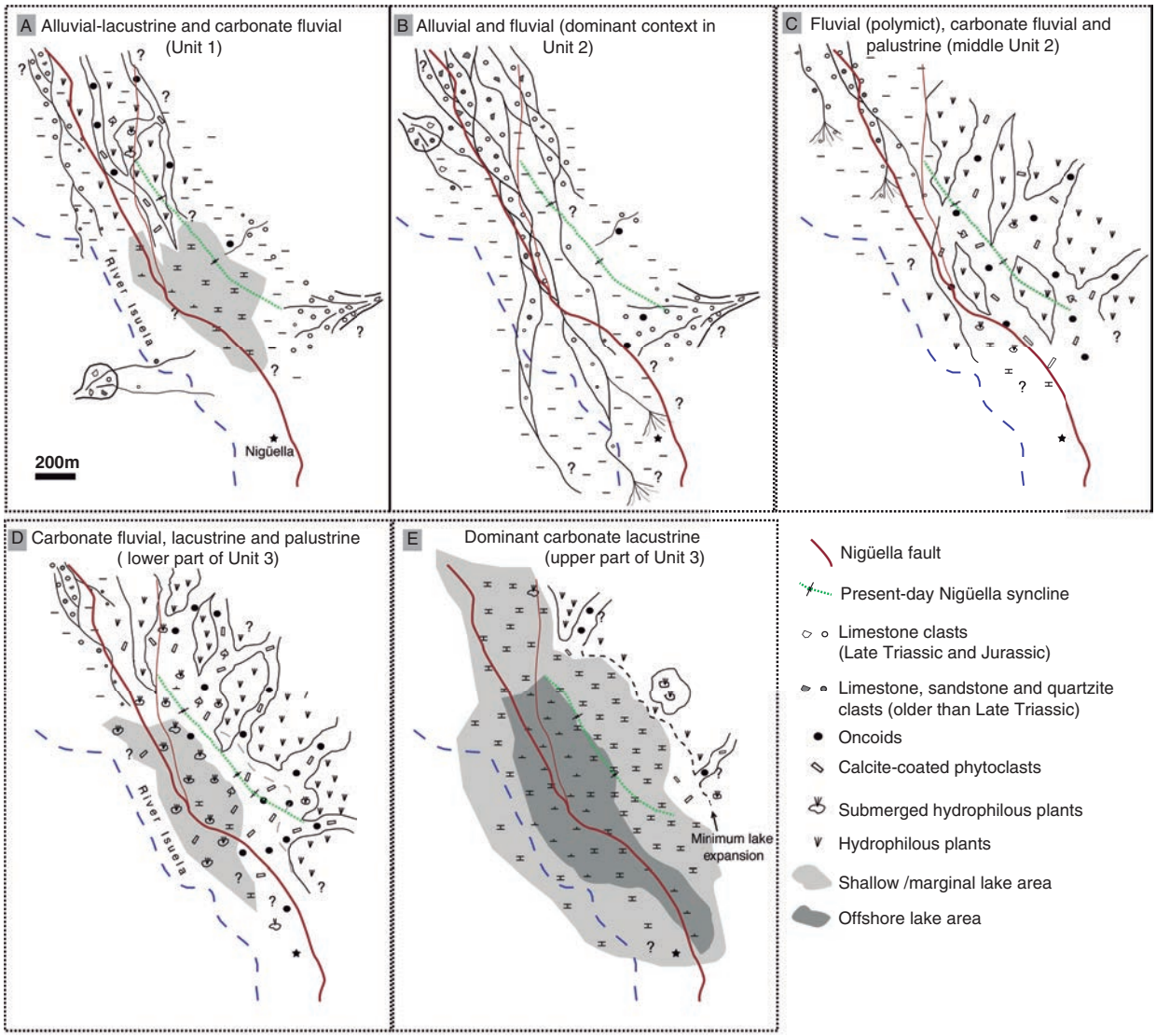

Figure 9.—Palaeogeographic sketches through time. A) Stage 1: Alluvial-lacustrine and carbonate fluvial environments (Unit 1). B) Stage 2: Alluvial and fluvial environments. The sketch represents the most common context during deposition of Unit 2. C) Fluvial (polymict), carbonate fluvial and palustrine environments representing deposition of the middle part of Unit 2. D) Stage 3: Carbonate fluvial, lacustrine and palustrine environments dominated by phytoclastic and oncolitic facies (lower part of Unit 3). E) Stage 4: Carbonate lake deposition, mainly with micritic limestones (upper part of Unit 3).

grains settled out and the water evaporation caused increased chemical concentration and then calcite precipitation occurred (mudstones and micritic limestones at the top of FA A2).

The overall evolution of Unit 1 in the southern area is fining-upward (Fig. 5). This evolution is linked to a general retrogradation of the sedimentary system. Most clastic sediment originated from Upper Triassic and Jurassic carbonate rocks, producing dominant monomict clastic lithofacies. The development of calcretes in Unit 1 suggests interruptions in sediment accretion that were linked to drought conditions (*e.g.*, Alonso-Zarza, 2003) before deposition of Unit 2. The fining upward sequences in Unit 1 (Fig. 5) represent retrogradation of the alluvial fans, followed by the development of small and shallow lakes, afterwards affected by long periods of drought (*cf.*, Sacristán-Horcajada *et al.*, 2016).

Depositional Stage 2 (Unit 2) was dominated by fluvial and less common alluvial deposition

(FA A1, A3 and B; Fig. 8). The most common situation (Fig. 9B) corresponded to a large braided fluvial system flowing southeastward, evolving from proximal-middle sectors in the north to middle-distal sectors in the south (*i.e.*, trunk system), with small alluvial fans from the east and northeast uplands (*i.e.*, marginal fans). Polymict gravels dominated throughout, which denotes the enlargement of the sediment source areas by addition of older rock outcrops. It is worth noting that sandstones are rare in this system, which denotes lack of maturity in the transport process (or in other words, short transport distance). This stage includes carbonate deposits approximately in the middle part of the unit that formed in shallow channels and pools, *i.e.*, a fluvial and fluvio-lacustrine setting in which hydrophilous plants, phytoclasts and oncoids were common. This situation coincided with a retrogradation of the trunk fluvial system (Fig. 9C). From this moment onward there is no record of marginal alluvial fan deposition.

The evolution of Unit 2 is cyclic (*i.e.*, fining upward and then coarsening upward), which is attributable to a regrogradation-progradation cycle of the sedimentary system. The sediment source area for all these fluvial and alluvial deposits were mainly the upper Triassic and Jurassic rocks in the south, and the lower and middle Triassic and Paleozoic rocks located towards the North (outside the studied area). Unit 2 represents a sharp palaeogeographic change respect to Unit 1. In the southern studied area, the lower half of Unit 2 includes both coarsening and fining-upward sequences (Fig. 5, section 3), with an increase in roundness of the clasts, an increase in fluvial versus alluvial processes (*e.g.*, channelled flows), and a decrease of calcrete formation in the uppermost deposits. The upper part of Unit 2 corresponds to a general progradation with extensive floodplains in the south. Together, these facts suggest an overall progradation of the fluvial system, providing the area with more water availability, *i.e.* due to more water availability, likely related to more humid conditions, since the end of deposition of Unit 1.

Unit 3 is dominated by carbonate deposits (Figs. 5, 9; FA D1 and D2, Fig. 8). Two distinct consecutive depositional stages are differentiated: one with phytoclastic and oncolitic limestones and marls (*Stage 3*, Fig. 9D) and another one with micritic, bioclastic limestones (*Stage 4*, Fig. 9E). A fluvio-lacustrine environment with Ca- and HCO_3^--rich water is proposed for Stage 3.

In the *Depositional stage 3* (lower part of Unit 3) shallow channels and ponded palustrine areas among them would be sites for hydrophilous plants to thrive; there, the submerged parts of plants would be coated by calcite (facies Lst). Breakage of these calcite-coated plants would cause formation of phytoclasts that would be deposited in nearby zones (facies Lph). Oncoids —mostly formed around plant stems fragments (already calcite-coated and non coated stems) and rare molluscs— and phytoclasts would form and accumulate in shallow, low-sinuosity channels (*e.g.*, as described by Vázquez-Urbez *et al.*, 2013). Other examples of oncoidal and associated carbonate deposits are also reported to occur mainly in fluvial and fluvial–lacustrine systems (Leinfelder & Hartkopf-Fröder, 1990; Zamarreño *et al.*, 1997; Hernández Gómez, 2000; Meléndez & Gómez-Fernández, 2000; Arenas *et al.*, 2007; Astibia *et al.*, 2012). The general channel flow in the studied area would run south-southwestwards, entering a shallow lake with marl and lime mud deposition. Marly deposits (*e.g.*, Fig.5, sections 2 and 3) represent periods of lake expansion, with thickest accumulation of marls in the south.

Depositional Stage 4 (upper part of Unit 3) is recorded by dominant micritic limestones (Lm) (Figs. 5, 6H), which formed by extensive lime mud lacustrine sedimentation in calm conditions (Fig. 9E). During this stage, the lacustrine deposition area expanded, as inferred from distribution of facies Lm outcrops. Outcrops in the studied area do not provide evidence of deposits corresponding to lake margin (*e.g.*, bioturbated or palustrine facies) or surrounding fluvial channels (*e.g.*, phytoclastic facies). Thus, the outcropping upper limestones of Unit 3 deposited in a relatively deeper, still and permanent water body compared to ponds in previous stages, and likely corresponding to close-lake conditions. The absence of wave structures and rarity of bioturbation features, along with the preservation of fossils and horizontal lamination vouch for such still and relatively deep context (*e.g.*, Cohen *et al*., 1997; Gierlowski-Kordesch, 2010; Vázquez-Urbez *et al.*, 2013).

Therefore, the overall sedimentary system in this area evolved from dominant alluvial-fluvial to dominant lacustrine carbonate environments

through time. This evolution is consistent with the basin expansion, in particular of the lacustrine area westward (*i.e.*, toward the passive margin; Figs. 2, 9), and is also consistent with the decrease in tectonic activity (compressive regime) through time, as discussed below. The decrease in tectonic activity, and thus in relief rejuvenation in the source areas, through the studied interval, *i.e.* after Unit 2 deposition, could favour fluvial incision uphill, downcutting the Mesozoic rocks, and then the outflow of ground water hosted in Jurassic carbonates (*i.e.*, springs), thus forming the source of Ca- and HCO_3^--saturated streams. This circumstance would explain the increase in carbonate deposition, in particular tufa, through time (*i.e.*, in Unit 3).

The characteristics of the dominant lacustrine deposition (micritic limestones with lamination, lacking bioturbation and current activity) suggests a hydrologically-closed lake, at least at the end of the deposition (*i.e.*, last depositional stage of Unit 3, Fig. 9E). Carbonate lake expansion would have been favoured by increasing water inputs into the basin, likely during a period of more humid climate conditions that may have coincided with the basin closure. The study of nearby fluvial and lacustrine outcrops and comparison with other close time-equivalent lacustrine records will help validate or reject this hypothesis.

Tecto-sedimentary evolution of the Nigüella sector in the Iberian Range

The proposed sedimentary evolution during the Miocene occurred under a compressive regime which is consistent with some observed geometrical features including: 1) the paralellism of the main cenozoic syncline fold axis (Nigüella syncline) and the main-fault cartographic trace (Nigüella fault) respect to the NW-SE trending southwest-vergent folds affecting upper Triassic and lower Jurassic strata, and 2) the close relationship between the spatial distribution of thickness variation of the studied units with respect to the hinge zone of the Nigüella syncline, and the related sedimentary environments. These facts suggest that sedimentation was controlled by accomodation space created during the syncline development on the hanging-wall Nigüella fault, as a result of the Miocene compression.

The Nigüella fault acted first under extensive regime as a normal fault, and then under compression producing a large fault-parallel buttress fault (the Nigüella syncline). The extensional history during early Jurassic times is deduced from regional data obtained from some other large-scale brittle structures linked to the deposition of the Cortes de Tajuña Formation in neighbouring areas of the Moncayo Massif (San Román & Aurell, 1992). Concerning the study zone, such extensional regime of the fault is compatible with the presence of extensional horses affecting the lower Jurassic strata (Figs. 2, 3A). On the contrary, the Nigüella fault's kinematics during the Cenozoic can be unambiguously deduced from the presence of hanging-wall southwest-vergent folds that are coaxial with respect to the main Mesozoic fault (Figs. 2, 3). In addition, in the northwesternmost studied area, the trace of the master fault bifurcates, and a secondary dextral strike-slip fault occurs.

In order to explain the tecto-sedimentary evolution of the Nigüella sector it is necessary to consider it within the Mesozoic framework of the NW Iberian Range. According to the above-mentioned evidence, the present-day configuration of the Neogene strata in this sector is consistent with two main tectonic stages (Fig. 10): 1) a lower Jurassic extensional stage responsible for a half-graben basin geometry, and 2) a Cenozoic shortening stage responsible for the formation of a fault-parallel buttress syncline.

The first tectonic stage is linked to the syn-sedimentary extensional tectonics related to the deposition of the Cortes de Tajuña Formation, Hettangian in age (Goy *et al*., 1976) (Fig. 10A), which has been recognized broadly in other sectors of the Iberian Range (San Roman & Aurell, 1992). This tectonic stage is well represented in the Nigüella area through both thickness variation of such Mesozoic unit in relation to the master Nigüella fault (Figs, 2, 3), and the presence of extensional structures (*i.e.*, horses like-structures) affecting the lower Jurassic units (Figs. 2, 3A).

The second tectonic stage recorded in the studied area involves the deformation of the previous extensional structures. During the Cenozoic compression, the NW-SE Mesozoic extensional master fault was folded and a hanging-wall syncline basin formed as a result of butressing of the NE block against

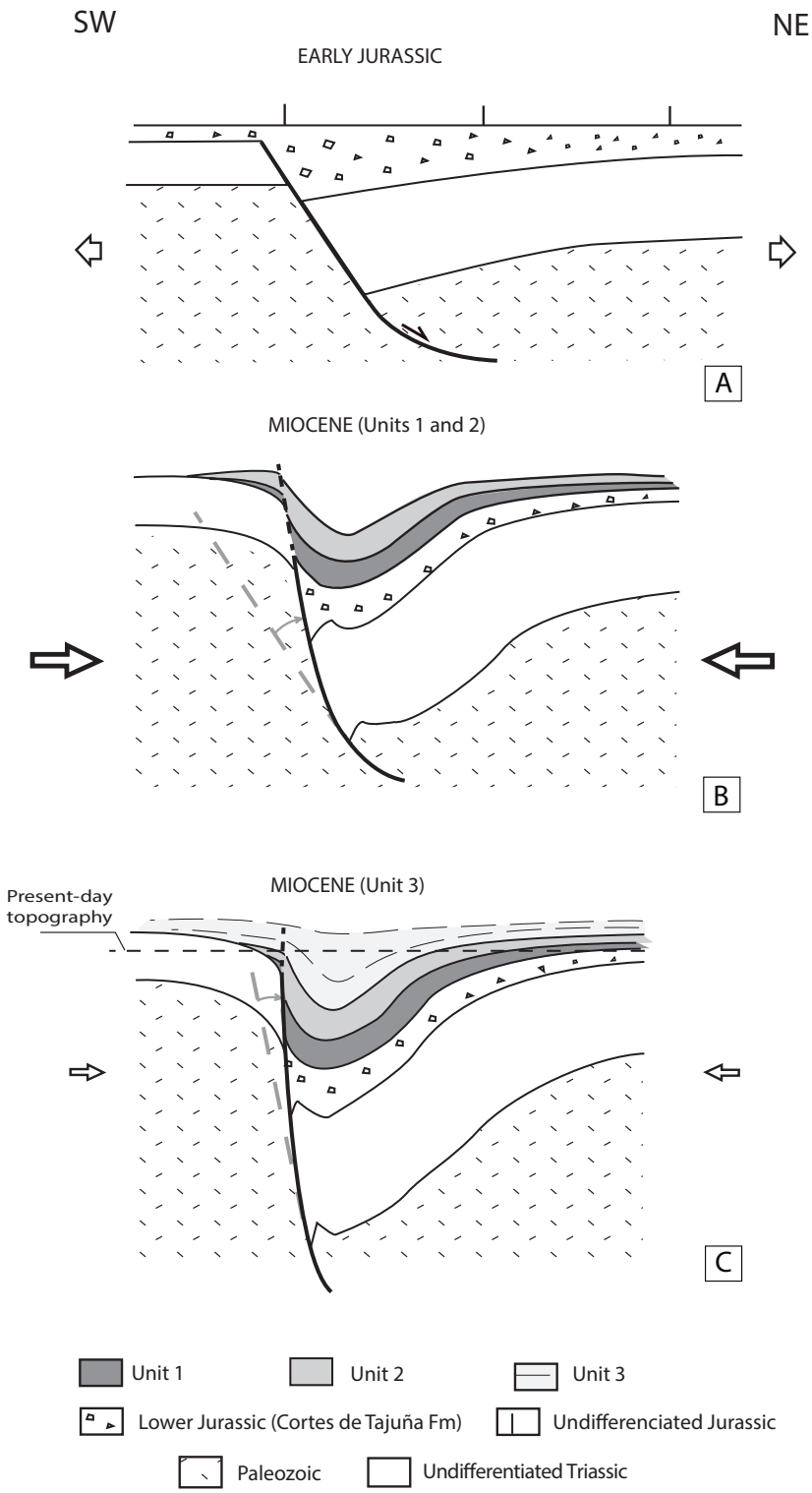

Figure 10.—Basin evolutionary model for the Nigüella sector (explanation in the text). Discontinuous gray lines in B and C indicate previous fault and rotation angle to present situation.

the verticalized fault. Similar examples have been described in different geological contexts (Butler, 1989; O'Dea & Lister, 1985; Simón, 2004; among others). Deposition of the studied Neogene succession took place in such a compressive scenario. Two Neogene deformation episodes can be differentiated. During the first one, deposition of predominantly clastic units (Units 1 and 2) took place, *e.g.* coinciding with deposits dated as Early Miocene from the fossils cited above, according to Ramírez del Pozo *et al.* (1978) (Fig. 10B). This first deformation pulse is not seen extensively through geometric devices, but can be inferred from the sedimentary evolution of the studied sequence. For instance, the change from fining-upward evolution in Unit 1 to Unit 2 represents a sharp grain-size jump that is accompanied by erosion (Fig. 5). Then, the cyclic fining-to-coarsening-upward evolution of Unit 2 corresponds to an overall increase in the intensity of tectonic activity, which resulted in a fault verticalization (Fig.10B). The second episode would represent waning tectonics, with the deposition of the predominantly carbonate sequence (Unit 3), likely during the end of compression later in the Miocene (Fig. 10C). In this stage a slight increase of the fault dip took place. The progressive decrease in tectonic intensity favoured lake expansion and resulted in a reduction of strata dip through time. The sedimentary features suit well other depositional fill contexts of extensional asymmetrical basins, such as those described in the Quaternary African east rift (Cohen *et al.*, 1997) or Upper Triassic-Lower Jurassic rift basins (Olsen *et al.*, 1990).

The proposed model explains the evolution of a portion of an intra-mountain basin in the northwestern sector of the Iberian Range, and shows the strong relationship between tectonics (formerly extensive and then sin-sedimentary compressive), drainage pattern evolution, sedimentation processes and climate changes. The results may help interpret the evolution of other complex basins whose sedimentary record is related to changes of relief and climate.

Conclusion

The sedimentary and structural study of a Cenozoic (likely Miocene) record in the northwestern Iberian Range and its relationship with the Mesozoic substrate allows the following considerations and conclusions:

- Compressive tectonics conditioned the occurrence of a hanging-wall syncline basin, the distribution and extent of Miocene lithofacies through space and time, and the location of depocentres.
- An ancient extensional fault, *i.e.*, the Nigüella fault, which play at the early Jurassic and was folded during the Cenozoic compression, promoted the formation of a hanging-wall syncline basin through buttressing of the NE block against the fault.
- Three tecto-sedimentary units are distinguished. Alluvial and fluvial deposition (dominant in Units 1 and 2) preceded extensive carbonate fluvial and lacustrine deposition (dominant in Unit 3). Calcrete development associated with alluvial facies suggest arid conditions during deposition of Units 1 and 2.
- Decreasing tectonic activity through the studied interval favoured fluvial incision uphill and then the outflow of ground water. Water was rich in Ca^{2+} and HCO^{-}_{3}, thus favouring widespread carbonate deposition (*i.e.*, Unit 3).
- Carbonate fluvial and lacustrine facies developed in a low-gradient depositional system that flowed southwestward and southward.
- Expansion of the lacustrine sedimentation at the end of the studied interval was conditioned by the increased humidity and likely the close character of the basin.

ACKNOWLEDGEMENTS

This work was financed by Project CGL2013-42867 of the Spanish Government and European Regional Funds. This work is a contribution of the Geotransfer research group (Aragón Government, FEDER and University of Zaragoza). Our gratitude to Dr. G. Pardo Tirapu for wise advise, and to reviewers Dr. I. Armenteros Armenteros and E. Arribas Mocoroa for pertinent corrections. We thank the *Servicio de Preparación de Rocas y Materiales Duros* (*Servicio General de Apoyo a la Investigación-SAI*) of the University of Zaragoza for their technical support. This contribution presents preliminary results of a IUCA research contract held by N. Santos Bueno.

References

Allen, J.R. (1982a). Sedimentary structures: their character and physical basis, volume I. Developments in Sedimentology 30A, Elsevier, Amsterdam, 593 pp.

Allen, J.R. (1982b). Sedimentary structures: their character and physical basis, volume II. Developments in Sedimentology 30B, Elsevier, Amsterdam, 663 pp.

Alonso-Zarza, A.M. (2003). Palaeoenvironmental significance of palustrine carbonates and calcretes in the geological record. Earth-Science Reviews, 60: 3-4, 261-298. https://doi.org/10.1016/S0012-8252(02)00106-X

Alonso-Zarza, A.M. & Arenas, C. (2004). Cenozoic calcretes from the Teruel Graben, Spain: microstructure, stable isotope geochemistry and environmental significance. Sedimentary Geology, 167: 91-108. https://doi.org/10.1016/j.sedgeo.2004.02.001

Aragonés Valls, E.; Hernández Samaniego, A.; Ramírez del Pozo, J. & Aguilar-Tomás, M.J. (1978). Mapa Geológico de España, E. 1: 50.000. Hoja nº 410 (La Almunia de Doña Godina). Instituto Geológico y Minero de España. Servicio de publicaciones – Ministerio de Industria y Energía, Madrid, 40 pp.

Arenas, C. (1993). Sedimentología y paleogeografía del Terciario del margen pirenaico y sector central de la Cuenca del Ebro (zona aragonesa occidental). Tesis Doctoral, Universidad de Zaragoza, 858 pp.

Arenas, C.; Pardo, G.; González, A. & Villena, J. (1989). El sistema aluvial de Cobatillas (Teruel): análisis de facies y evolución del estilo fluvial. Revista de la Sociedad Geológica de España 2: 41–54.

Arenas, C. & Pardo, G. (1999). Latest Oligocene-Late Miocene lacustrine systems of the north-central part of the Ebro Basin (Spain): sedimentary facies model and palaeogeographic synthesis. Palaeogeography, palaeoclimatology, palaeoecology, 151: 127- 148. https://doi.org/10.1016/S0031-0182(99)00025-5

Arenas, C.; Gutiérrez, F.; Osácar, C. & Sancho, C. (2000). Sedimentology and geochemistry of fluvio-lacustrine tufa deposits controlled by evaporite solution subsidence in the central Ebro depresión, NE spain. Sedimentology, 47: 883-909. https://doi.org/10.1046/j.1365-3091.2000.00329.x

Arenas, C.; Cabrera, L. & Ramos, E. (2007). Sedimentology of tufa facies and continental microbialites from the Palaeogene of Mallorca Island (Spain). Sedimentary Geology, 197: 1-27. https://doi.org/10.1016/j.sedgeo.2006.08.009

Arenas-Abad, C.; Vázquez-Urbez, M.; Pardo-Tirapu, G. & Sancho-Marcén, C. (2010). Fluvial and associated carbonate deposits. In: Carbonates in continental settings (Alonso-Zarza, A.M. & Tanner, L.H., Eds.), Developments in Sedimentology, 61: 133-175.

Armenteros, I.; Daley, B. & García, E. (1997). Lacustrine and palustrine facies in the Bembridge Limestone (late Eocene, Hampshire Basin) of the Isle of Wight, southern England, Palaeogeography, Palaeoclimatology, Palaeoecology, 128: 111–132. https://doi.org/10.1016/S0031-0182(96)00108-3

Arp, G.; Reimer, A. & Reitner, J. (2001). Photosynthesis-induced biofilm calcification and calcium concentrations in Phanerozoic oceans. Science, 292(5522): 1701-1704. https://doi.org/10.1126/science.1057204

Ashley, G.M. (2002). Glaciolacustrine environments. In: Modern and Past Glacial Environments. (Menzies, J., Ed.), Butterworth-Heinemann, Oxford, 335-359. https://doi.org/10.1016/B978-075064226-2/50014-3

Astibia, H.; López-Martínez, N.; Elorza, J. & Vicens, E. (2012). Increasing size and abundance of microbialites (oncoids) in connection with the K/T boundary in nonmarine environments in the South Central Pyrenees. Geologica Acta, 10: 209–226.

Butler, R. W. H. (1989). The influence of pre-existing basin structure on thrust system evolution in the western Alps. In: Inversion Tectonics (Cooper M.A. & Williams, G.D., Eds.). Special Publication of the Geological Society, London, 44: 105-122. https://doi.org/10.1144/GSL.SP.1989.044.01.07

Cabrera, L; Cabrera, M.; Gorchs, R. & de las Heras, F.X. (2002). Lacustrine basin dynamics and organo-sulphur compound origin in a carbonate-rich lacustrine system (Late Oligocene Mequinenza Formation, SE Ebro Basin, NE Spain). Sedimentary Geology, 148: 289-317. https://doi.org/10.1016/S0037-0738(01)00223-8

Cabrera, L.; Arbués, P.; Cuevas, J.L.; Garcés, M.; López-Blanco, M.; Marzo, M. & Valero, L. (2011). Integrated analysis of the depositional fill in evolving –marine to continental– forelands: Advances in the easterna Ebro basin (Eocene-Early Miocene, NE Spain). In: Pre-Meeting Field Trips Guidebook (Arenas, C.; Pomar, L. & Colombo, F., Eds.), 28th IAS Meeting, Sociedad Geológica de España, Geo-Guías, 7: 151–198.

Cohen, A.S.; Talbot, M.R.; Awramick, S.M.; Dettman, D.L. & Abell, P. (1997). Lake level and paleoenvironmental history of Lake Tanganyika, Africa, as inferred from late Holocene and modern stromatolites. Geological Society of America Bulletin, 109: 444–460. https://doi.org/10.1130/0016-7606(1997)109<0444:LLAPHO>2.3.CO;2

Dunham, R.J. (1962). Classification of Carbonate rocks according to depositional texture. In: Classification of Carbonate Rocks (Ham, W.E. Ed.), Memories of the American Association of Petroleum Geologists, 1, Tulsa, 108–121.

Embry, A.F. & Klovan, J.E. (1971): A late Devonian reef tract on northeastern Banks Island, NW Territories. Bulletin of Canadian Petroleum Geology, 19: 730–781.

Ezquerro, L. (2017). El sector norte de la cuenta neógena de Teruel: tectónica, clima y sedimentación. PhD Thesis, Universidad de Zaragoza, 494 pp.

Fielding, C.R.; Lagarry, H.E.; Lagarry, L.A.; Bailey, B.E., & Swinehart, J.B. (2007). Sedimentology of the Whiteclay Gravel Beds (Ogallala Group) in northwestern Nebraska, USA: structurally controlled drainage promoted by early Miocene uplift of the Black Hills Dome. Sedimentary Geology, 202: 58–71. https://doi.org/10.1016/j.sedgeo.2006.12.009

Gabaldón, V. (Dir.); Lendínez, A.; Ferreiro, E.; Ruiz, V.; López de Alda, F.; Valverde, M.; Lago San José, M.; Meléndez, A.; Pardo, G.; Ardevol, L.; Villena, J.; Pérez, A.; González, A.; Hernández, A.; Álvaro, M.; Leal, M.C.; Aguilar Tomás, M.; Gómez, J.J. & Carls P. (1991). Mapa Geológico de España, 1:200,000, sheet 40 (Daroca). Instituto Tecnológico y GeoMinero de España. Servicio de Publicaciones, Madrid, 239 pp.

Gierlowski-Kordesch, E.H. (2010). Lacustrine carbonates. In: Carbonates in continental settings (Alonso-Zarza, A.M. & Tanner, L.H., Eds.), Developments in Sedimentology, 61: 1-101.

Goy, A.; Gómez, J.J., & Yébenes, A. (1976). El Jurásico de la Cordillera Ibérica (mitad norte): I. Unidades litoestratigráficas. Estudios Geológicos 32: 391-423.

Hernández Gómez, J.M. (2000). Sedimentología, paleogeografía y relaciones tectónica/sedimentación de los sistemas fluviales, aluviales y palustres de la cuenca rift de Aguilar (Grupo Campo, Jurásico superior-Cretácico inferior de Palencia, Burgos y Cantabria). PhD Thesis, Universidad del País Vasco, 324 pp.

Hernández-Samaniego, A.; Aragonés, E.; Ramírez, J. & Aguilar, T. (1978). Mapa Geológico de España, 1:50,000. Sheet 409 (Calatayud). Instituto Geológico y Minero de España. Servicio de Publicaciones – Ministerio de Industria y Energía, Madrid, 44 pp.

Kumar, R.; Suresh, N.; Sangode, S.J. & Kumaravel, V. (2007). Evolution of the Quaternary alluvial fan system in the Himalayan foreland basin: implications for tectonic and climatic decoupling. Quaternary International, 159: 6–20. https://doi.org/10.1016/j.quaint.2006.08.010

Leinfelder, R.R. & Hartkopf-Fröder, C. (1990). In situ accretion mechanism of convavo-convex lacustrine oncoids ("swallow nests") from the Oligocene of the Mainz Basin, Rhineland, Fluvial Research Group. Sedimentology, 37: 287–301. https://doi.org/10.1111/j.1365-3091.1990.tb00960.x

López-Gómez, J. & Arche, A. (1997). The Upper Permian Boniches Conglomerates Formation: evolution from alluvial fan to fluvial system environments and accompanying tectonic and climatic controls in the southeast Iberian Ranges, central Spain. Sedimentary Geology, 114: 267–294. https://doi.org/10.1016/S0037-0738(97)00062-6

Meléndez, N. & Gómez-Fernández, J.C. (2000). Continental deposits of the Eastern Cameros Basin (Northern Spain) during Tithonian-Berriasian time. In: Lake Basins Through Space and Time (Gierlowski-Kordesch, E.H. & Kelts, K.R., Eds), American Association of Petroleum Geologists, Studies in Geology, 46: 263–278.

Miall, A.D. (1977). A review of the braided river depositional environment. Earth Science Reviews, 13: 1–62. https://doi.org/10.1016/0012-8252(77)90055-1

Miall, A.D. (1978). Lithofacies types and vertical profile models in braided river deposits: a summary. In: Fluvial Sedimentology. 5. (Miall, A.D., Ed.). Canadian Society of Petroleum Geologists Memoir, 597–604.

Miall, A.D. (2006). The geology of fluvial deposits. Springer-Verlag Berlin Heidelberg, New York, 441 pp. https://doi.org/10.1007/978-3-662-03237-4

O´Dea, M. G. & Lister, G. S. (1995). The role of ductility contrast and basement architecture in the structural evolution of the Crystal Creek block, Mount Isa Inlier, NW Queensland, Australia. Journal of Structural Geology, 17 (7): 949-960. https://doi.org/10.1016/0191-8141(94)00117-I

Olivé Davó, A.; del Olmo, P.; Portero, J.M.; Carls, P.; Sdzuy, K.; Collande, C.V. Kolb, S.; Teyssen, T.; Gutiérrez, M.; Puidgdefábregas, C.; Giner, J.; Portero, J.M.; Aguilar, M.J.; Leal, M.C.; Goy, A.; Coma, M.J.; Adrover, R. & Gabaldón, V. (Dir.) (1983). Mapa Geológico de España, Sheet 438 (Paniza). 1:50,000. Instituto Geológico y Minero de España. Servicio de publicaciones – Ministerio de Industria y Energía, Madrid, 80 pp.

Olsen, P. E. (1990) Tectonic, climatic, and biotic modulation of lacustrine ecosystems—examples from Newark supergroup of eastern North America, in B. J. Katz, ed., Lacustrine Basin Exploration, American Association of Petroleum Geologists, Memoir 50: 209-224.

Ordóñez, S. & García del Cura, M.A. (1983). Recent and Tertiary fluvial carbonates in Central Spain. In: Ancient and Modern Fluvial Systems (Collinson, J.D. & Lewin,J.), International Association of Sedimentologists Special Publication, 6: 485-497.

Pedley, H.M. (1990). Classification and environmental models of cool freshwater tufas. Sedimentary Geology, 68(1-2): 143-154. https://doi.org/10.1016/0037-0738(90)90124-C

Pedley, M. (2009). Tufas and travertines of the Mediterranean region: a testing ground for freshwater carbonate concepts and developments. Sedimentology, 56: 221-246. https://doi.org/10.1111/j.1365-3091.2008.01012.x

Pentecost, A. (2005). Travertine. Springer Science & Business Media. 445 pp.

Pettijohn, F. P.; Potter, P. E. & Siever, R. (1973). Sand and sandstones. Springer-Verlag, New York-Heidelberg-Berlin, 618 pp. https://doi.org/10.1007/978-1-4615-9974-6

Platt, N.H. (1989). Lacustrine carbonates and pedogenesis: sedimentology and origin of palustrine deposits from

the Early Cretaceous Rupelo Formation, W Cameros Basin, N Spain. Sedimentology, 36: 665–684. https://doi.org/10.1111/j.1365-3091.1989.tb02092.x

Porter, R.J. & Gallois, R.W. (2008). Identifying fluvio-lacustrine intervals in thick playa-lake successions: an integrated sedimentology and ichnology of arenaceous members in the mid–Late Triassic Mercia Mudstone Group of south-west England UK. Palaeogeography, Palaeoclimatology, Palaeoecology, 270: 381–398. https://doi.org/10.1016/j.palaeo.2008.07.020

Ramírez del Pozo, J.; Aguilar Tomás, M.; del Olmo Zamora, P.; Aragonés Valls, E. & Hernández Samaniego, A. (1978). Mapa geológico de España, 1:50,000, Sheet 381 (Illueca). Instituto Geológico y Minero de España. Servicio de publicaciones – Ministerio de Industria y Energía, Madrid, 39 pp.

Riding, R. (1991a). Classification of Microbial Carbonates. In: Calcareous Algae and Stromatolites (Riding, R., Ed.). Springer-Verlag, Berlin, 21–51. https://doi.org/10.1007/978-3-642-52335-9_2

Riding R. (1991b). Calcified Cyanobacteria. In: Calcareous Algae and Stromatolites (Riding, R., Ed.). Springer-Verlag, Berlin, 55–87. https://doi.org/10.1007/978-3-642-52335-9_3

Robador Moreno, A.; Hernández Samaniego, A.; Léndinez González, A.; Gonzalo Gutiérrez, R.; Ramajo Moreno, A.; Cabra Gil, P. & Pérez García, A. (2006). Mapa geológico de España, 1:50,000, Sheet 382 (Épila). Instituto Geológico y Minero de España. Servicio de Publicaciones – Ministerio de Industria y Energía, Madrid, 163 pp.

Sacristán-Horcajada, S.; Arribas, M.E. & Mas, R. (2016). Pedogenetic calcretes in early syn-rift alluvial systems (Upper Jurassic, West Cameros Basin), northern Spain. Journal of Sedimentary Research, 86: 268-286. https://doi.org/10.2110/jsr.2016.30

San Román, J. & Aurell, M. (1992). Palaeogeographical significance of the Triassic-Jurassic unconformity in the north Iberian basin (Sierra del Moncayo, Spain). Palaeogeography, Palaeoclimatology, Palaeoecology, 99: 101-117. https://doi.org/10.1016/0031-0182(92)90009-T

Santos-Bueno, N. (2015). Estratigrafía y tectónica del Terciario en el sector Nigüella-Mesones de Isuela (Zaragoza). Trabajo Fin de Grado, Universidad de Zaragoza, 39 pp.

Sanz Rubio, E. (1999). Análisis de los sistemas deposicionales carbonáticos y evaporíticos del Neógeno de la cuenca de Calatayud. PhD Thesis, Universidad Complutense de Madrid, 579 pp.

Shukla, U.K. (2009). Sedimentation model of gravel-dominated alluvial piedmont fan, Ganga Plain, India. International Journal of Earth Sciences, 98: 443–459. https://doi.org/10.1007/s00531-007-0261-4

Simón, J.L. (2007). Superposed buckle folding in the eastern Iberian Chain, Spain. Journal of Structural Geology, 26: 1447-1464. https://doi.org/10.1016/j.jsg.2003.11.026

Vázquez-Urbez, M. (2008). Caracterización y significado ambiental de depósitos tobáceos neógenos en la Cuenca del Ebro. Comparación con ambientes cuaternarios (PhD Thesis, Universidad de Zaragoza). 542 pp.

Vázquez-Urbez, M.; Arenas, C. & Pardo, G. (2012). A sedimentary facies model for stepped, fluvial tufa systems in the Iberian Range (Spain): The Quaternary Piedra and Mesa valleys. Sedimentology, 59: 502–526. https://doi.org/10.1111/j.1365-3091.2011.01262.x

Vázquez-Urbez, M.; Arenas, C.; Pardo, G. & Pérez-Rivarés, J. (2013). The effect of drainage reorganization and climate on the sedimentologic evolution of intermontane lake systems: The final fill stage of the Tertiary Ebro Basin (Spain). Journal of Sedimentary Research, 83(8): 562-590. https://doi.org/10.2110/jsr.2013.47

Vera, J. A. (Ed.). (2004). Geología de España. SGE-IGME, Madrid, 890 pp.

Wright, V.P. & Tucker, M.E. (1991). Calcretes. The international association of Sedimentologists. Blackwell Scientific Publications, Oxford, Reprint Series 2, 380 pp. https://doi.org/10.1002/9781444304497

Zamarreño, I.; Anadón, P. & Utrilla, R. (1997). Sedimentology and isotopic composition of Upper Palaeocene to Eocene non-marine stromatolites, eastern Ebro Basin, NE Spain. Sedimentology, 44: 159–176. https://doi.org/10.1111/j.1365-3091.1997.tb00430.x